1 **Title:** Fluorescent Bioaerosol Particle, Molecular Tracer, and Fungal Spore Concentrations during Dry
2   and Rainy Periods in a Semi-Arid Forest
3

5 **Authors:** Marie Ila GOSSELIN[1,2], Chathurika M Rathnayake[3], Ian Crawford[4], Christopher Pöhlker[2],
6   Janine Fröhlich-Nowoisky[2], Beatrice Schmer[2], Viviane R. Després[5], Guenter Engling[6], Martin
7   Gallagher[4], Elizabeth Stone[3], Ulrich Pöschl[2], and J. Alex Huffman[1*]
8
9 [1]Department of Chemistry and Biochemistry, University of Denver, Denver, Colorado, USA
10 [2]Max Planck Institute for Chemistry, Multiphase Chemistry and Biogeochemistry Departments, Mainz,
11   Germany
12 [3]Department of Chemistry, University of Iowa, Iowa City, IA 52246, USA
13 [4]Centre for Atmospheric Science, SEAES, University of Manchester, Manchester, UK
14 [5]Institute of General Botany, Johannes Gutenberg University, Mainz, Germany
15 [6]Division of Atmospheric Sciences, Desert Research Institute, Reno, NV, USA
16
17 * Correspondence to: alex.huffman@DU.edu

Abstract:

Bioaerosols pose risks to human health and agriculture and may influence the evolution of mixed-phase clouds and the hydrological cycle on local and regional scales. The availability and reliability of methods and data on the abundance and properties of atmospheric bioaerosols, however, are rather limited. Here we analyze and compare data from different real-time Ultraviolet Laser/Light Induced Fluorescence (UV-LIF) instruments with results from a culture-based spore sampler and offline molecular tracers for airborne fungal spores in a semi-arid forest in the Southern Rocky Mountains of Colorado. Commercial UV-APS (Ultraviolet Aerodynamic Particle Sizer) and WIBS-3 (Wideband Integrated Bioaerosol Sensor, Version 3) instruments with different excitation and emission wavelengths were utilized to measure fluorescent aerosol particles (FAP) during both dry weather conditions and periods heavily influenced by rain. Seven molecular tracers of bioaerosols were quantified by analysis of total suspended particle (TSP) high-volume filter samples using High Performance Anion Exchange Chromatography with Pulsed Amperometric Detection (HPAEC-PAD). From the same measurement campaign, Huffman et al. (2013) previously reported dramatic increases in total and fluorescent particle concentrations during and immediately after rainfall and also showed a strong relationship between the concentrations of FAP and ice nuclei (Huffman et al., 2013; Prenni et al., 2013). Here we investigate molecular tracers and show that during rainy periods the atmospheric concentrations of arabitol (35.2 ± 10.5 ng m^{-3}) and mannitol (44.9 ± 13.8 ng m^{-3}) were 3-4 times higher than during dry periods. During and after rain the correlations between FAP and tracer mass concentrations were also significantly improved. Fungal spore number concentrations on the order of 10^4 m^{-3}, accounting for 2-4% of TSP mass during dry periods and 17-23% during rainy periods, were obtained from scaling the tracer measurements and from multiple analysis methods applied to the UV-LIF data. Endotoxin concentrations were also enhanced during rainy periods, but showed no correlation with FAP concentrations. Average mass concentrations of erythritol, levoglucosan, glucose, and (1→3)-β-D-glucan in TSP samples are reported separately for dry and rainy weather conditions. Overall, the results indicate that UV-LIF measurements can be used to infer fungal spore concentrations, but substantial development of instrumental and data analysis methods seems required for improved quantification.

1. Introduction

Primary biological aerosols particles (PBAP) are of keen interest within the scientific community, partially because methods for their quantification and characterization are advancing rapidly (Huffman and Santarpia, 2016; Sodeau and O'Connor, 2016). The term PBAP, or equivalently bioaerosol, generally comprises several classes of airborne biological particles including viruses, bacteria, fungal spores, pollen and their fragments (Després et al., 2012; Fröhlich-Nowoisky, 2016). Fungal spores are of particular atmospheric interest because they can cause a variety of deleterious health effects in humans, animals, and agriculture, and it has been shown that they can represent a significant fraction of total organic aerosol emissions (Deguillaume et al., 2008; Gilardoni et al., 2011; Madelin, 1994), especially in tropical regions (Elbert et al., 2007; Huffman et al., 2012; Pöschl et al., 2010; Zhang et al., 2010). Current estimates of the atmospheric concentration of fungal spores range from 10^0 to more than $10^4\,m^{-3}$ (Frankland and Gregory, 1973; Gregory and Sreeramulu, 1958; Heald and Spracklen, 2009; Hummel et al., 2015; Sesartic and Dallafior, 2011). Fungal spores may also impact the hydrological cycle as giant cloud condensation nuclei (GCCN) or as ice nuclei (IN) (Haga et al., 2013; Morris et al., 2013; Sesartic et al., 2013). Additionally, several classes of bioaerosols and their constituent components, such (1→3)-β-D-glucan and endotoxins, have been implicated in respiratory distress and allergies (Burger, 1990; Douwes et al., 2003; Laumbach and Kipen, 2005; Linneberg, 2011; Pöschl and Shiraiwa, 2015). For example, asthma and allergies have shown notable increases during thunderstorms due to elevated bioaerosol concentrations (Taylor and Jonsson, 2004) especially when attributed to fungal spores (Allitt, 2000; Dales et al., 2003).

Molecular tracers have long been utilized as a means of aerosol source tracking (Schauer et al., 1996; Simoneit and Mazurek, 1989; Simoneit et al., 2004). In recent years, analysis of molecular tracers has been utilized for the quantification of PBAP in atmospheric samples and has been compared, for example, with results from microscopy (Bauer et al., 2008a) and culture samples (Chow et al., 2015b; Womiloju et al., 2003). Three organic molecules have been predominately utilized as unique tracers of fungal spores: ergosterol, mannitol, and arabitol. The majority of atmospherically relevant fungal spores are released by active wet discharge processes common in *Ascomycota* and *Basidiomycota*, meaning that the fungal organism actively ejects spores at a time most advantageous for the spore dispersal and germination processes, often when relative humidity (RH) is high (Ingold, 1971). While there are several mechanisms of active spore emission (e.g. Buller's drop (Buller, 1909) and osmotic pressure canons (Ingold, 1971)), they each involve the secretion of fluid containing hygroscopic compounds, such as arabitol, mannitol, potassium and chloride ions, as well as other solutes (Elbert et al., 2007), released near the site of spore growth. When the spores are ejected, some of the fluid adheres to the spores and becomes aerosolized. Several of these secreted compounds are thought to enter the atmosphere linked uniquely with spore emission processes, and so these tracers have been used to estimate atmospheric concentrations of fungal spores. Arabitol and mannitol are both sugar alcohols (polyols) that serve as energy stores for the spore (Feofilova, 2001). Arabitol is unique to fungal spores and lichen, while mannitol is present in fungal spores, lichen, algae, and higher plants (Lewis and Smith, 1967). Ergosterol is found within the cell membranes of fungal spores (Weete, 1973) and has been used as an ambient fungal spore trace (Di Filippo et al., 2013; Miller and Young, 1997). Comparing the seasonal trends of arabitol and mannitol with ergosterol, Burshtein et al. (2011) showed positive correlations between arabitol or mannitol and ergosterol only in the spring and autumn suggesting that the source of these polyols is unlikely to be solely fungal in origin or that the amount of each compound emitted varies considerably between species type and season. While ergosterol has been directly linked to fungal spores in the air, ergosterol is prone to photochemical degradation and is difficult to analyze and quantify directly. Quantification of ergosterol typically requires chemical derivatization by silylation before analysis via gas chromatography (Axelsson et al., 1995; Burshtein et al., 2011; Lau et al., 2006). In contrast, analysis of sugar alcohols by ion chromatography involves fewer steps and has been successfully applied to monitor seasonal variations of atmospheric aerosol concentration at a number of sites (Bauer et al., 2008a; Caseiro et al., 2007; Yang et al., 2012; Yttri et al., 2011a; Zhang et al., 2010; Zhang et al.,

2015) including pg m^{-3} levels in the Antarctic (Barbaro et al., 2015). By measuring spore count and tracer concentration in parallel at one urban and two suburban sites in Vienna, Austria Bauer et al. (2008a) estimated the amount of each tracer per fungal spore emitted. Potassium ions have also been linked to emission of biogenic aerosol (Pöhlker et al., 2012b) and are co-emitted with fungal spores, however, application of potassium as a fungal tracer is uncommon because it is predominantly associated with biomass burning (Andreae and Crutzen, 1997). Additionally, (1→3)-β-D-glucan (fungal spores and pollen) and endotoxins (gram-negative bacteria) have also been widely used to measure other bioaerosols (Andreae and Crutzen, 1997; Cheng et al., 2012; Rathnayake et al., 2016b; Stone and Clarke, 1992).

The direct detection of PBAP has historically been limited to analysis techniques that require culturing or microscopy of the samples. These systems are time-consuming, costly, and often substantially undercount biological particles by an order of magnitude or more (Gonçalves et al., 2010; Pyrri and Kapsanaki-Gotsi, 2007). The sampling methods associated with these measurements also offer relatively low time resolution and low particle size resolution. Recently, techniques utilizing ultraviolet laser/light-induced fluorescence (UV-LIF) for the real-time detection of PBAP have been developed and are being utilized by the atmospheric community for bioaerosol detection. Thus far, the most widely applied LIF instruments for ambient PBAP detection have been the Ultraviolet Aerosol Particle Sizer (UV-APS; TSI Inc. Model 3314, St. Paul, MN) and the Wideband Integrated Bioaerosol Sensor (WIBS; University of Hertfordshire, Hertfordshire, UK, now licensed to Droplet Measurement Technologies, Boulder, CO, USA). Both of these commercially available instruments can provide information in real-time about particle size and fluorescence properties of supermicron atmospheric aerosols. Characterization and co-deployment of these instruments over the past ten years has expanded the knowledge base regarding how to analyze and utilize the information provided from these instruments (Crawford et al., 2015; Healy et al., 2014; Hernandez et al., 2016; Huffman et al., 2013; Perring et al., 2015; Pohlker et al., 2013; Pöhlker et al., 2012a; Ruske et al., 2016), though the interpretation of UV-LIF results from individual particles is complicated by interfering material that is not biological in nature (Gabey et al., 2010; Huffman et al., 2012; Lee et al., 2010; Saari et al., 2013; Toprak and Schnaiter, 2013).

Here we present analysis of atmospheric concentrations of arabitol and mannitol in relation to results from real-time, ambient particle measurements reported by UV-APS and WIBS. We interrogate these relationships as they pertain to rain conditions (rainfall and RH) that have previously been shown to increase the concentrations of fluorescent aerosols and ice nuclei (Crawford et al., 2014; Huffman et al., 2013; Prenni et al., 2013; Schumacher et al., 2013; Yue et al., 2016). Active wet discharge of ascospores and basidiospores has frequently been reported to correspond with increased RH (Elbert et al., 2007), and fungal spore concentration has also been shown to increase after rain events (e.g. Jones and Harrison, 2004). Here we estimate airborne fungal concentrations in a semi-arid forest environment utilizing a combination of real-time fluorescence methods, molecular fungal tracer methods, and direct-to-agar sampling and culturing as parallel surrogates for spore analysis. This study of ambient aerosol represents the first quantitative comparison of real-time aerosol UV-LIF instruments with molecular tracers or culturing.

2. Methods

2.1 Sampling site

Atmospheric sampling was conducted as a part of the BEACHON-RoMBAS (Bio-hydro-atmosphere interactions of Energy, Aerosols, Carbon, H$_2$O, Organics, and Nitrogen – Rocky Mountain Biogenic Aerosol Study) field campaign conducted at the Manitou Experimental Forest Observatory (MEFO) located 48 km northwest of Colorado Springs, Colorado (2370 m elevation, 39$^{\rm o}$ 06' 0" N, 105$^{\rm o}$ 5' 03" W) (Ortega et al., 2014). The site is located in the central Rocky Mountains and is representative of semi-arid montane pine forested regions of North America. During BEACHON-RoMBAS a large,

148 international team of researchers conducted an intensive set of measurements from 20 July to 23 August
149 2011. A summary of results from the campaign are published in the BEACHON campaign special issue
150 of Atmospheric Chemistry and Physics[1]. All the data reported here were gathered from instruments and
151 sensors located within a <100 m radius (Fig. 1).
152
153 **2.2 Online fluorescent instruments**
154 UV-APS and WIBS-3 (Model 3; University of Hertfordshire) instruments were operated
155 continuously as a part of the study, and particle data were integrated to five-minute averages before
156 further analysis. The UV-APS was operated under procedures defined in previous studies (Huffman et al.,
157 2013; Schumacher et al., 2013). A total suspended particle (TSP) inlet head ~5.5 m above ground,
158 mounted above the roof of a climate-controlled, metal trailer, was used to sample aerosol directed towards
159 the UV-APS. Bends and horizontal stretches in the 0.75 inch tubing were minimized to reduce losses of
160 large particles (Huffman et al., 2013) . The UV-APS detects particles between 0.5-20 µm and records
161 aerodynamic particle diameter and integrated total fluorescence (420-575 nm) after pulsed excitation by a
162 355 nm laser (Hairston et al., 1997). Both UV-APS and WIBS instruments report information about
163 particle number concentration, but it is instructive here to show results in particle mass for comparison
164 between all techniques. Total particle number size distributions (irrespective of fluorescence properties)
165 obtained from the UV-APS and WIBS were converted to mass distributions assuming spherical particles
166 of unit particle mass density, unless otherwise stated, as a first approximation. Total particle concentration
167 values (in $\mu g\ m^{-3}$) were obtained for each five-minute period by integrating over the size range $0.5 - 15$
168 µm, and these mass concentration values were averaged over the length of the filter sampling periods.
169 Uncertainty in mass concentration values reported here is influenced by assuming a single value for
170 particle mass density and because of slight dissimilarities between size bins of UV-APS and WIBS
171 instruments at particle sizes above 10 µm that dominate particle mass.
172
173 A WIBS-3 was used to continuously sample air at a site ~50 m from the UV-APS trailer and 1.3
174 m above the ground. Briefly, the diameter of individual particles sampled by the WIBS is estimated by
175 the intensity of the elastic side-scatter from a continuous wave 635 nm diode laser and analyzed by a Mie
176 scattering model (Foot et al., 2008; Kaye et al., 2005). Particles that pass through the diode laser activate
177 two optically-filtered Xenon flash lamps. The first lamp excites the particle at 280 nm and the second at
178 370 nm. Emission from the 280 nm excitation is filtered separately for two PMTs, one which detects in a
179 band at 320-400 nm and the other in a band at 410-650 nm. These excitation and emission wavelengths
180 result in a total of three channels of detection: λ_{ex} 280 nm, λ_{em} 320 – 400 nm (FL 1 or Channel A); λ_{ex} 280
181 nm, λ_{em} 410 – 650 nm (FL 2 or Channel B); and λ_{ex} 370 nm, λ_{em} 410– 650 nm (FL 3 or Channel C)
182 (Crawford et al., 2014). Individual particles are considered fluorescent here if they exceed fluorescent
183 thresholds for any channel, as defined as the average of a "forced trigger" baseline plus 3 standard
184 deviations (σ) of the baseline measurement (Gabey et al., 2010).
185
186 WIBS particle-type analysis is utilized to define types of particles that have specific spectral
187 patterns. As defined by Perring et al. (2015), the 3 different fluorescent channels (FL1, FL2, and FL3) can
188 be combined to produce 7 unique fluorescent categories. Observed fluorescence in channel FL1 alone, but
189 without any detectable fluorescence in Channel FL2 or FL3, categorizes a particle as type A. Similarly,
190 observed fluorescence in channels FL2 or FL3, but in no other channels, places a particle in the B or C
191 categories, respectively. Combinations of fluorescence in these channels, such as a particle that exhibits
192 fluorescence in both FL1 and FL2 categorizes a particle as type AB and so on for a possible seven particle
193 types as summarized in Figure S1.
194

---

[1]http://www.atmos-chem-phys.net/special_issue247.html

195 As a separate tool for particle categorization, the University of Manchester has recently developed and
196 applied a hierarchical agglomerative cluster analysis tool for WIBS data, which they have previously
197 applied to the BEACHON-RoMBAS campaign (Crawford et al., 2014; Crawford et al., 2015; Robinson et
198 al., 2013). Here we utilize clusters derived from WIBS-3 data as described by Crawford et al. (2015).
199 Cluster data presented here was analyzed with the Open Source Python package FastCluster (Mullner,
200 2013). Briefly, hierarchical agglomerative cluster analysis was applied to the entire data set and each
201 fluorescent particle was uniquely clustered into one of 4 groups. Cluster 1, assigned by Crawford et al.
202 (2015) as fungal spores, displayed a 1.5-2 µm mode and a daily peak in the early morning that paralleled
203 relative humidity (Schumacher et al., 2013). Clusters 2, 3, and 4 have strong, positive correlations with
204 rainfall and exhibit size modes that peak at <1.2 µm and were initially described by Crawford et al. as
205 bacterial particles. Here we have summed Clusters 2-4 to a single group referred to as Cl_{Bact}, for
206 simplicity when comparing with molecular tracers. It should be noted that assignment of name and origin
207 (e.g. fungal spores or bacteria) to clusters is approximate and does not imply naming accuracy or particle
208 homogeneity. Each cluster likely contains an unknown fraction of contaminating particles, but the clusters
209 are beneficial to group particles more selectively than using fluorescent intensity alone. For more details
210 see Robinson et al. (2013) and Crawford et al. (2015).
211
212 The WIBS-3 utilized here has since been superseded by the WIBS-4 (Univ. Hertfordshire, UK)
213 and WIBS-4A (Droplet Measurement Technologies, Boulder, Colorado). One important difference
214 between the models is that the optical chamber design and filters of the WIBS-4 models were updated to
215 enhance the overall sensitivity of the instrument (Crawford et al., 2014). Additionally, slight differences
216 in detector gain between models and individual units can impact the relative sensitivity of the
217 fluorescence channels. This may result in differences in fluorescent channel intensity between instrument
218 models, as will be discussed later.
219
220 2.3 High volume sampler
221 Total suspended particle samples were collected for molecular tracer and molecular genetic
222 analyses using a high volume sampler (Digitel DHA-80) drawing 1000 L min^{-1} through 15 cm glass fiber
223 filters (Macherey-Nagel GmbH, Type MN 85/90, 406015, Düren, Germany) over a variety of sampling
224 times ranging from 4-48 h (supplemental Table S1). The sampler was located <50 m from each of the
225 UV-LIF instruments described here, approximately between the WIBS-3 and UV-APS. Prior to sampling
226 all filters were baked at 500 °C for 12 h to remove DNA and organic contaminants. Samples were stored
227 in pre-baked aluminum bags after sampling at -20 °C for 1-30 days and then at -80 °C after overnight,
228 international transport cooled on dry ice. Due to the low vapor pressure of the molecular tracers analyzed
229 loss due to volatilization is considered unlikely (Zhang et al., 2010). 36 samples were collected during the
230 study, in addition to handling field blanks and operational field blanks. Handling blanks were acquired by
231 placing a filter into the sampler and immediately removing, without turning on the air flow control.
232 Operational blanks were placed into the sampler and exposed to 10 seconds of air flow.
233
234 2.4 Slit Sampler
235 A direct-to-agar slit sampler (Microbiological Air Sampler STA-203, New Brunswick Scientific
236 Co, Inc., Edison, NJ) was used to collect culturable airborne fungal spores. The sampler was placed ~2 m
237 above ground on a wooden support surface with 5 cm x 5 cm holes to allow air flow both up and down
238 through the support structure. Sampled air was drawn over the 15 cm diameter sampling plate filled with
239 growth media at a flow rate of 28 L min^{-1} for sampling periods of 20 to 40 min. Growth media (malt
240 extract medium) was mixed with antibacterial agents (40 units streptomycin, Sigma Aldrich; 20 units
241 ampicillin, Fisher Scientific) to suppress bacterial colony growth. Plates were prepared several weeks in
242 advance and stored in a refrigerator at ca. 4 °C until used for sampling. Before each sampling period, all
243 surfaces of the samplers were sterilized by wiping with isopropyl alcohol. Handling and operational
244 blanks were collected to verify that no fungal colonies were being introduced by handling procedures. 14
245 air samples were collected over 20 days and immediately moved to an incubator (Amerex Instruments,

246 Incumax IC150R) set at 25 °C for 3 days prior to counting fungal colonies formed. Each colony, present
247 as a growing dot on the agar surface, is assumed to have originated as one colony forming unit (CFU; i.e.
248 fungal spore) deposited onto the agar by impaction during sampling. The atmospheric concentration of
249 CFU per air volume was calculated using the sampler air flow. Further discussion of methods and initial
250 results from the slit sampler were published by Huffman et al. (2013).
251
252 **2.5 Offline filter analyses**
253
254 *2.5.1 Carbohydrate analysis*
255 Approximately 1/8 of each frozen filter was cut for carbohydrate analysis using a sterile
256 technique, meaning that scissors were cleaned and sterilized and cutting was performed in a positive-
257 pressure laminar flow hood. In order to precisely determine the fractional area of the filter to be analyzed,
258 filters were imaged from a fixed distance above using a camera and compared to a whole, intact filter.
259 Using ImageJ software (Rasband and ImageJ, 1997), the area of each filter slice showing particulate
260 matter (PM) deposit was referenced to a whole filter, and thereby the amount of each filter utilized could
261 be determined. The total PM mass was not measured and so this technique allowed for an estimation of
262 the fraction of each sample used for the analysis, which corresponds to the fraction of PM mass deposited.
263 The uncertainty on the filter area fraction is estimated at 2%, determined as the percent of variation in the
264 area of the filter edge (no PM deposit) as compared to the total filter area.
265
266 Water soluble carbohydrates were extracted from quartz filter samples and analyzed following the
267 procedure described by Rathnayake et al. (2016a). A total of 36 samples were analyzed along with field
268 and lab blanks. All lab and field blanks fell below method detection limits. Extraction was performed by
269 placing the filter slice into a centrifuge tube that had been pre-rinsed with Nanopure^{TM} water (resistance >
270 18.2 MΩ cm^{-1}; Barnstead EasyPure II, 7401). A volume of 8.0 mL of Nanopure^{TM} water was added to the
271 filter in the centrifuge tube to extract water-soluble carbohydrates. Samples were then exposed to rotary
272 shaking for 10 min at 125 rpm, sonication for 30 min at 60 Hz (Branson 5510, Danbury, CT, US), and
273 rotary shaking for another 10 min. After shaking, the extracted solutions were filtered through a 0.45 μm
274 polypropylene syringe filter (GE Healthcare, UK) to remove insoluble particles, including disintegrated
275 filter pieces. One 1.5 mL aliquot of each extracted solution was analyzed for carbohydrates within 24
276 hours of extraction. A duplicate 1.5 mL aliquot was stored in a freezer and analyzed, if necessary due to
277 lack of instrument response or invalid calibration check, within 7 days of extraction. Analysis of
278 carbohydrates was done using a High Performance Anion Exchange Chromatography System with Pulsed
279 Amperometric Detection (HPAEC-PAD, Dionex ICS 5000, Thermo Fisher, Sunnyvale, CA, USA).
280 Details of the instrument specifications and quality standards for carbohydrate determination are available
281 in Rathnayake et al. (2016). Calibration curves for mannitol, levoglucosan, glucose (Sigma-Aldrich),
282 arabitol and erythritol (Alfa Aesar) were generated with seven points each, ranging in aqueous
283 concentration from 0.005 ppm to 5 ppm. The method detection limits for mannitol, levoglucosan, glucose,
284 arabitol, and erythritol were 2.3, 2.8, 1.6, 1.0, and 0.6 ppb, respectively. Method detection limits were
285 determined as 3σ of analyte concentrations recovered from seven spiked filter samples (Rathnayake et al.,
286 2016a). All calibration curves were checked daily using a standard solution to ensure all concentration
287 values were within 10% of the known value. Failure to maintain a valid curve resulted in recalibration of
288 the instrument.
289
290 *2.5.2 DNA analysis*
291 Methods and initial results from DNA analysis from these high volume filters were published by
292 Huffman et al. (2013). Briefly, fungal diversity was determined by previously optimized methods for
293 DNA extraction, amplification, and sequence analysis of the internal transcribed spacer regions of
294 ribosomal genes from the high volume filter samples (Fröhlich-Nowoisky et al., 2012; Fröhlich-
295 Nowoisky et al., 2009). Upon sequence determination, fungal sequences were compared with known
296 sequences using the Basic Local Alignment Search Tool (BLAST) at the National Center for

297 Biotechnology (NCBI) and identified to the lowest taxonomic rank common to the top BLAST hits after
298 chimeric sequences had been removed. When sequences displayed >97% similarity, they were grouped
299 into operational taxonomic units (OTUs).
300
301 *2.5.3 Endotoxin and glucan analysis*
302   Sample preparation for quantification of endotoxin and $(1\rightarrow3)$-β-D-glucan included extraction of
303 5 punches ($0.5\ cm^2$ each) of the quartz filters with 5.0 mL of pyrogen-free water (Associates of Cape Cod
304 Inc., East Falmouth, MA, USA), utilizing an orbital shaker (300 rpm) at room temperature for 60 min,
305 followed by centrifuging for 15 min (1000 rpm). One-half mL of supernatant was submitted to a kinetic
306 chromogenic limulus amebocyte lysate (Chromo-LAL) endotoxin assay (Associates of Cape Cod Inc.,
307 East Falmouth, MA, USA) using a ELx808IU (BioTek Instrument Inc., Winooski, VT, USA) incubating
308 absorbance microplate reader. For $(1\rightarrow3)$-β-D-glucan measurement, 0.5 mL of 3 N NaOH was added to
309 the remaining 4.5 mL of extract and the mixture was agitated for 60 min. Subsequently, the solution was
310 neutralized to pH 6–8 by addition of 0.75 mL of 2 N HCl. After centrifuging for 15 min $(1\rightarrow3)$-β-D-
311 glucan concentration was determined in the supernatant using the Glucatell® LAL kinetic assay
312 (Associates of Cape Cod, Inc., East Falmouth, MA). The minimum detection limits (MDLs) and
313 reproducibility were 0.046 Endotoxin Units (EU) $m^{-3} \pm 6.4\%$ for endotoxin and 0.029 ng $m^{-3} \pm 4.2\%$ for
314 $(1\rightarrow3)$-β-D-glucan, respectively. Laboratory and field blank samples were analyzed as well, with lab
315 blank values being below detection limits, while field blank values were used to subtract background
316 levels from sample data. More details about the bioassays can be found elsewhere (Chow et al., 2015a).
317
318 **2.6 Meteorology and wetness sensors**
319 Meteorological data were recorded by a variety of sensors located at the site. Precipitation was recorded
320 by a laser optical disdrometer (PARticle SIze and VELocity "PARSIVEL" sensor; OTT Hydromet
321 GmbH, Kempton, Germany) and separately by a tipping bucket rain gauge. The disdrometer provides
322 precipitation occurrence, rate, and physical state (rain or hail) by measuring the magnitude and duration
323 of disruption to a continuous 780 nm laser that was located in a tree clearing (Fig. 1), while the tipping
324 bucket rain gauge measures a set amount of precipitation before tipping and triggering an electrical pulse.
325 A leaf wetness sensor (LWS; Decagon Devices, Inc., Pullman, WA), provided a measurement of
326 condensed moisture by measuring the voltage drop across a leaf surface to determine a proportional
327 amount of water on or near the sensor. Additional details of these measurements can be found in Huffman
328 et al. (2013) and Ortega et al. (2014).
329
330 **3. Results and Discussion**
331
332 **3.1 Categorization and characteristic differences of Dry and Rainy periods**
333   Increases in PBAP concentration have been frequently associated with rainfall (e.g. Bigg et al.,
334 2015; Faulwetter, 1917; Hirst and Stedman, 1963; Jones and Harrison, 2004; Madden, 1997). Fungal
335 polyols have also been reported to increase after rain and have been used as indicators of increased fungal
336 spore release (Liang et al., 2013; Lin and Li, 2000; Zhu et al., 2015). Recently it was shown that the
337 concentration of fluorescent aerosol particles (FAP) measured during BEACHON-RoMBAS increased
338 dramatically during and after periods of rain (Crawford et al., 2014; Huffman et al., 2013; Schumacher et
339 al., 2013) and that these particle were associated with high concentrations of ice nucleating particles that
340 could influence the formation and evolution of mixed-phase clouds (Huffman et al., 2013; Prenni et al.,
341 2013; Tobo et al., 2013). It was observed that a mode of smaller fluorescent particles (2-3 μm) appeared
342 during rain episodes, and several hours after rain ceased a second mode of slightly larger fluorescent
343 particle (4-6 μm) emerged, persisting for up to 12 h (Huffman et al., 2013). The first mode was
344 hypothesized to result from mechanical ejection of particles due to rain splash on soil and vegetated
345 surfaces, and the second mode was suggested as actively emitted fungal spores (Huffman et al., 2013).
346 While the UV-APS and WIBS each provide data at high enough time resolution to see subtle changes in
347 aerosol concentration, the temporal resolution of the chemical tracer analysis was limited to 4-48 h

periods defined by the collection time of the high volume sampler. To compare the measurement results across the sampling platforms, UV-LIF measurements were averaged to the lower time resolution of the filter sampler periods, and the periods were grouped into three broad categories: Rainy, Dry, and Other, as will be defined below.

Time periods were wetness-categorized in two steps: first at 15 min resolution and then averaged for each individual filter sample. During the first stage of categorization each 15 min period was categorized into one of four groups: rain, post-rain, dry, or other. To categorize each filter period, an algorithm was established utilizing UV-APS fluorescent particle fraction and accumulated rainfall. The ratio of integrated number of fluorescent particles to total particles was used as a proxy for the increased emission of biological particles. Figure 2a presents a time series of the size-resolved fluorescent particle concentration, showing increases during rain periods in dark red. A relatively consistent diurnal cycle of increased FAP concentration in the 2-4 μm range is apparent almost every afternoon, which corresponds to near daily afternoon rainfall during approximately the first half of the measurement period. Disdrometer and tipping bucket rainfall measurements were each normalized to unity and summed to produce a more robust, unitless measure of rainfall rate, because it was observed that often only one of the two systems would record a given light rain event. If a point was described by total rainfall accumulation greater than 0.201 it was flagged as rain. A point was flagged as post-rain if it immediately followed a rain period and also exhibited a fluorescent particle fraction greater than 0.08. The purpose of this category was to reflect the observation that sustained, elevated concentrations of FAP persisted for many hours even after the rain rate, RH, and leaf wetness returned to pre-rain values. The only measurement that adequately reflected this scenario was of the fluorescent particles measured by UV-APS and WIBS instruments. The post-rain flag was continued until the fluorescent particle fraction fell below 0.08 or if it started to rain again (with calculated rain values greater than 0.201). Points were flagged as dry periods if they exhibited rainfall accumulation and fluorescent particle fraction below the thresholds stated above. Several periods were not easily categorized by this system and were considered in a fourth category as other. This occurred when fluorescent particle fraction above the threshold value was observed with no discernable rainfall.

Once wetness categories were assigned by the algorithm at 15 min resolution, each high volume filter sample was categorized by a similar nomenclature, but using only three categories. These were defined as Dry, Rainy (combination of rain and post rain categories), or Other based on the relative time fraction in each of the four original 15 min categories. For each sample, if a given category represented more than 50% of the 15 min periods, the sample was assigned to that category. Despite the effort to categorize samples systematically, several sample periods (5 of 35) appeared mis-categorized by looking at FAP concentration, rainfall, RH, and leaf wetness in more detail. In some circumstances, this was because light rainfall produced observable increases in FAP, but without exceeding the rainfall threshold. Or in other circumstances a period of rainfall occurred at the very end or just before the beginning of a sample, and so the many-hour period was heavily influenced by aerosol triggered by a period of rain just outside of the sample time window. As a result, several samples were manually re-categorized as described here. Samples 20 and 21 (Table S1) were four-hour samples that displayed high relative humidity and rainfall, thus samples were originally characterized as Rainy. This period was described by an extremely heavy rain downpour (7.5 mm in 15 min), however, that seemingly placed the samples in a different regime of rain-aerosol dynamics than the other Rainy samples and so these two samples were moved to the Other category. Sample 23, originally Rainy, presented a FAP fraction marginally above the 0.08 threshold, but visually displayed a trend dissimilar to other post-rain periods and so was re-categorized as Dry. Sample 28 showed no obvious rainfall, but the measurement team observed persistent fog in three consecutive mornings (Samples 25, 27, 28), and the concentration of fluorescent particles (2-6 μm) suggested a source of particles not influenced by rain, and so this Rainy sample was re-categorized as Other. Sample 38 displayed a fluorescent number ratio just below the threshold value, and was first categorized as Dry, however, the measurement team observed post-rain periods at the beginning and end of the sample, so the sample were re-categorized as Other. For all samples other than these five, the

399 categorization was determined using the majority (> 0.50) of the 15 min periods. In no cases other than
400 the five that were re-categorized was the highest category fraction less than 0.50 of the sample time. Note
401 that we have chosen to capitalize Rainy, Dry, and Other to highlight that we have rigorously defined the
402 period using the characterization scheme described above and to separate the nomenclature from the
403 general, colloquial usage of the terms. Wetness category assignment for each high volume filter sample
404 period is shown in Figure 2 as a background color (brown for Dry samples, green for Rain–influenced
405 samples, and pink for Other samples) and Table S1.
406
407   To validate the qualitative differences between wetness categories described in the last section,
408 we present observations about each of these groupings. First, we organized the WIBS data according to
409 the particle categories introduced by Perring et al. (2015). By this method, every fluorescent particle
410 detected by the WIBS can be defined uniquely into one of seven categories (i.e. A, AB, ABC and so on).
411 By plotting the relative fraction of fluorescent particles described by each particle type, temporal
412 differences between measurement periods can be observed, as shown in Figure 2e. To a first
413 approximation, this analysis style allows for coarse discrimination of particle types. For example, a given
414 population of particles would ideally exhibit a consistent fraction of particles present in the different
415 particle categories as a function of time. By this reasoning, sample periods categorized as Dry (most of
416 the latter half of the study; brown bars in Fig. 2) would be expected to have a self-consistent particle type
417 trend, whereas sample periods categorized as Rainy (most of the first half of the study; green bars in Fig.
418 2) would have a self-consistent particle type trend, but different from the Dry samples. This is broadly
419 true. During Rainy periods as seen in Figure 3a, there is a relatively high fraction (> 65%) of ABC
420 particles (light blue) and a relatively low fraction (< 15%) in BC (purple) and C (yellow) type particles,
421 suggesting heavy influence from the FL1 channel. In contrast, during Dry periods the fraction of ABC
422 particles (light blue) is reduced (<25%) while BC (purple) and C (yellow) type particles increase in
423 relative fraction (>30% and >40%, respectively) suggested a diminished influence of FL1 channel.
424
425   It is important to note a few caveats here. First, the ability of the WIBS to discriminate finely
426 between PBAP types is relatively poor and it is still unclear exactly how different particle types would
427 appear by this analysis method. Particles of different kinds and from different sources are likely
428 convolved into a single WIBS particle type, which could either soften or enhance the relationships with
429 rain discussed here. Second, the assignment of particle types is heavily size-dependent and sensitive to
430 subtle instrument parameters, and so it is unclear how different instruments would present similar particle
431 types. For example, Hernandez et al. (2016) used two WIBS instruments and found differences in relative
432 fraction of particle categories for samples aerosolized in the lab. They reported fungal spores to be
433 predominately A, AB, and ABC type particles, whereas Rainy sample periods suggested to have heavy
434 fungal spore influence by Huffman et al. (2013) show predominantly C, BC, and ABC particle fraction.
435 These discrepancies may be due to the comparison of ambient particles to laboratory-grown cultures. The
436 highly controlled environment of a laboratory may not always accurately represent the humidity
437 conditions in which fungal spore release occurs in this forest setting (Saari et al., 2015). This could impact
438 the fluorescence properties of fungal spore particles that have different amounts of adsorbed or associated
439 water (Hill et al., 2009; 2013; 2015). More likely, however, is that the WIBS-3 used here exhibits
440 differences in fluorescence sensitivity from the WIBS-4A used by Hernandez et al. (2016). Even a slight
441 increase in sensitivity in the FL3 channel with respect to the FL1 or FL2 channels could explain the shift
442 here towards particles with C-type fluorescence. One piece of evidence for this is the quantitative
443 comparison of particle measurements presented by the UV-APS and WIBS-3 instruments co-deployed
444 here (Fig. 4). The number concentration of particle exhibiting fluorescence above the FL2 baseline of the
445 WIBS-3 is approximately consistent with the number of fluorescent particles measured by the UV-APS,
446 and significantly below the concentration of FL3 particles. The UV-APS number concentration shows the
447 highest correlation with the WIBS-3 FL2 channel: during Rainy periods, $R^2= 0.70$; Dry, $R^2=0.82$; Other,
448 $R^2 =0.92$. These observations are in stark contrast to the trends reported by Healy et al. (2014) that the
449 UV-APS fluorescent particle concentration correlated most strongly with the WIBS-4 FL3 and that the

450   number concentration of FL3 was the lowest out of all three channels. Given that the FL3 channel of the
451   WIBS and the UV-APS probe cover similar excitation and emission wavelengths it is expected that these
452   two channels should correlate well. Based on these data, we suggest that the WIBS-3 utilized here may
453   present a very different particle type break-down than if a WIBS-4 had been used. So, while caution is
454   recommended when comparing the relative break-down of WIBS particle categories shown here (Fig. 3)
455   with other studies, the data are internally self-consistent, and comparing qualitative differences between,
456   e.g. Rainy and Dry periods is expected to be robust. The main point to be highlighted here is that there is
457   indeed a qualitative difference in particles present in the three wetness categories, as averaged and shown
458   in Figure 3a, which generally supports the effort to segregate these samples.

459

460   Further evidence that there is a qualitative difference in the three wetness categories is shown
461   using molecular genetic analysis (Figs. 3b, c). The analysis of fungal DNA sequences from 21 of the high
462   volume samples found 406 operational taxonomic units (OTUs), belonging to different fungal classes and
463   phyla. When organized by wetness type it was observed that 106 of these occurred only on Rainy
464   samples, 148 of these occurred on Dry samples, and 37 on Other samples, with some fraction occurring in
465   overlaps of each (Fig. 3c). This shows that the number of OTUs observed uniquely in either the Rainy or
466   Dry periods is greater than the number of OTUs present in both wetness types, suggesting that the fungal
467   communities in each grouping are relatively distinct. Further, Figure 3b shows a break-down of fungal
468   taxonomic groupings for each wetness group. This analysis shows that there is a qualitative difference in
469   taxonomic break-down between periods of Rainy and Dry. Specifically, during Dry periods there is an
470   increased fraction of *Pucciniomycetes* (green bar, Fig. 3c), *Chytridiomycetes* (yellow), *Sordariomycetes*
471   (orange), and *Eurotiomycetes* (pink) when compared to the Rainy periods.

472

473   **3.2 Atmospheric mass concentration of arabitol, mannitol, and fungal spores**
474   To estimate fungal spore emission to the atmosphere, the concentration of arabitol and mannitol
475   (Fig. 5a, b, Table S2) in each aerosol sample was averaged for all samples in each of the three wetness
476   categories. The average concentration of arabitol collected on Rainy TSP samples (35.2 ± 10.5 ng m^{-3})
477   increased by a factor of 3.3 with respect to Dry samples, and the average mannitol concentration on Rainy
478   samples was higher by a factor of 3.7 (44.9 ± 13.8 ng m^{-3}). Figures 5a, b show the concentration
479   variability for each wetness category, observed as the standard deviation from the distribution of
480   individual samples. For each polyol, there is no overlap in the ranges shown, including the outliers of the
481   Rainy and Dry category, suggesting a definitive and conceptually distinct separation between dry periods
482   and those influenced by rain. The concentrations observed during Other periods is between those of the
483   Dry and Rainy averages, as expected, given the difficulty in confidently assigning these uniquely to one
484   of these categories. The observations here are roughly consistent with previous reports of polyol
485   concentration, despite differences in local fungal communities and concentrations. For example,
486   Rathnayake et al. (2016a) observed 30.2 ng m^{-3} arabitol and 41.3 ng m^{-3} mannitol in PM$_{10}$ samples
487   collected in rural Iowa, USA. In addition, Zhang et al. (2015) reported arabitol and mannitol
488   concentrations in PM$_{10}$ samples of 44.0 and 71.0 ng m^{-3}, respectively, from a study in the mountains on
489   Hainan Island off the coast of Southern China. More recently, Yue et al. (2016) studied a rain event in
490   Beijing and observed increased polyol concentrations at the onset of the rain. The observed mannitol
491   concentration (45 ng m^{-3}) was approximately consistent with observations reported here and with
492   previous reports, while the arabitol concentration values observed were approximately an order of
493   magnitude lower (0.3 ng m^{-3}).

494

495   The square of the correlation coefficient (R^2) here between concentration values of arabitol and
496   mannitol during Rainy samples is very high (0.839; Table 1) suggesting that arabitol and mannitol
497   originated primarily from the same source, likely active-discharge fungal spores. The correlation is
498   similar to the 0.87 R^2 reported by Bauer et al. (2008a) and the 0.93 R^2 reported by Graham et al. (2003).
499   In contrast, the same correlation between mannitol and arabitol concentrations, but for Dry samples is
500   relatively low (0.312). This is consistent with reports that arabitol can be used more specifically as a spore

tracer, but that mannitol has additional atmospheric sources besides fungal spores. The same correlation was also performed between arabitol or mannitol and other molecular tracers (endotoxins and $(1{\rightarrow}3)$-β-D-glucan), but all R^2 value were less than 0.43, suggesting that the endotoxins and glucans analyzed were not emitted uniquely from the same sources as arabitol and mannitol.

Results from the two UV-LIF instruments were averaged over high volume sample periods, and a correlation analysis was performed between tracer mass and fluorescent particle mass showing positive correlations in all cases. The FAP mass from the UV-APS shows high correlation with the fungal polyols during Rainy periods, with R^2 of 0.732 and 0.877 for arabitol and mannitol, respectively (Table 2; Figure 5c, d). The same tracers correlate poorly with the UV-APS during Dry conditions. This is expected, because *ascomycetes* and *basidiomycetes* emitted by wet discharge methods are the only fungal spores reported to be associated with arabitol and mannitol (Elbert et al., 2007; Feofilova, 2001; Lewis and Smith, 1967). This high correlation suggests that the UV-APS does a good job of detecting these wet-discharge spores, and corroborates previous statements that particles detected in ambient air by the UV-APS are often predominately fungal spores (Healy et al., 2014; Huffman et al., 2013; Huffman et al., 2012). In contrast, the low slope value and the poor correlation during Dry periods suggest that the UV-APS is also sensitive to other kinds of particles, as designed. The small positive x-offset (FAP mass; Table S2, Figs. 5c,d) during Rainy periods is likely due to particles that are too weakly fluorescent to be detected and counted by the UV-APS, which is consistent with observations made in Brazil (Huffman et al., 2012).

Particle mass from WIBS Cl1, assigned to fungal spores (Crawford et al., 2015), also correlate strongly with the same two molecular tracers. Both Rainy periods (R^2 0.824) and Dry periods (R^2 0.764) correlate well with arabitol (Fig. 5e), while mannitol (Fig. 5f) only shows a strong correlation during the Rainy periods (R^2 0.799). Mannitol is a common polyol in higher plants while arabitol is only found in fungal spores and lichen (Lewis and Smith, 1967). So the strong correlation of each polyol with UV-LIF mass during Rainy periods when actively-discharged spores are expected to dominate and the similarly strong correlations associated with arabitol suggest that the Cl1 cluster does a reasonably good job of selecting fungal spore particles. The poor correlation between mannitol and Cl1 during dry periods illustrates that the background mannitol concentration is likely not due to fungal spores alone, but has contribution from other higher plants that contain mannitol. Particle concentrations detected by individual WIBS channels and in the other cluster were also compared with polyol concentrations, but each correlation is relatively poor compared to that with respect to Cl1. As seen in Table 2 and Figures S2-S3, correlations in FL1, 2, and 3 with arabitol are poor (<0.4) in the Dry category and good ($0.4 < R^2 < 0.7$) in the Rainy category. For mannitol, all the UV-LIF instruments show high correlation (>0.7) in all cases. This is likely due to mannitol being a non-specific tracer and suggests that the majority of UV-LIF particles observed during all periods was dominated by PBAP.

3.3 Estimated number concentration of fungal spore aerosol

Bauer et al. (2008a) reported measurements of fungal spore number concentration in Vienna, Austria using epifluorescence microscopy and also measured fungal tracer mass collected onto filters in order to estimate the mass of arabitol (1.2 to 2.4 pg spore^{-1}) and mannitol (0.8 to 1.8 pg spore^{-1}) associated with each emitted spore. Bauer et al. (2008a) and Yttri et al. (2011b) reported ratios of mannitol to arabitol of approximately 1.5 ($\pm$ standard deviation of 26%) and 1.4 $\pm$ 0.3, respectively. Our measurements show slightly lower ratios of mannitol to arabitol, but that the ratio is dependent on wetness category; Rainy, 1.29 $\pm$ 0.17; Dry, 1.12 $\pm$ 0.23; and Other, 1.24 $\pm$ 0.54. The mannitol to arabitol ratio would be expected to vary as a function of fungal population present in the aerosol, whether between different wetness periods at a given location or between different physical localities.

Using the approximate mid-point of the Bauer et al. (2008a) reported ranges, 1.7 pg mannitol per spore and 1.2 pg arabitol per spore, atmospheric number concentrations of spores collected onto the high

552 volume filters were calculated from the polyol mass concentrations measured here. Based on these values,
553 and assuming all polyol mass originated with spore release, the mass concentration averages (Fig. 5) were
554 converted to fungal spore number concentrations (Fig. 6). The trends of spore concentration averages are
555 the same as with the polyol mass, because the numbers were each multiplied by the same scalar value.
556 After doing so, the analysis reveals an estimated spore concentration during Dry periods of 0.89×10^4 ($\pm$
557 0.21) spores m^{-3} using the arabitol concentration and 0.70×10^4 (± 0.19) spores m^{-3} using the mannitol
558 concentration (Table 3). The estimated concentration of spores increased approximately three-fold during
559 Rainy periods to 2.9×10^4 (± 0.8) spores m^{-3} (arabitol estimate) and 2.6×10^4 (± 0.8) spores m^{-3} (mannitol
560 estimate) (Figure 6a, b). These estimates match well with estimates reported by Spracklen and Heald
561 (2014), who modeled the concentration of airborne fungal spores across the globe as an average of $2.5 \times$
562 10^4 spores m^{-3}, with approximately 0.5×10^4 spores m^{-3} over Colorado.
563
564   The UV-LIF instruments discussed here are number-counting techniques and in this instance have
565 been applied as spore counters. As a first approximation, each particle detected by the UV-APS was
566 assumed to be a fungal spore with the same properties used in the assumptions by Bauer et al. (2008a).
567 Figures 6d, e, g, h show correlations of fungal spore number concentration estimated from polyol mass on
568 the y-axes and from UV-LIF measurements on the x-axes. The first, and most important observation is
569 that the estimated fungal spore concentration from each technique is on the same order of magnitude, 10^4
570 m^{-3}. Looking at individual correlations reveals a finer layer of detail. These results show that the number
571 concentration of fungal spores estimated by the UV-APS is greater than the number of fungal spores
572 estimated by the tracers, as evidenced by slope values of approximately 0.2 and 0.35 for Rainy and Dry
573 conditions, respectively (Tables S3, Figs. 6d, e). Again, this suggests that the UV-APS detects fungal
574 spores as well as other types of fluorescent particles. The R^2 values (~0.5) during Rainy periods indicate
575 that the additional source of particles detected by the UV-APS is likely to have a similar source, such as
576 PBAP mechanically ejected from soil and vegetative surfaces with rain-splash (Huffman et al., 2013).
577 The magnitude of the over-estimation is higher during Dry periods, which would be expected because
578 Rainy periods exhibited much higher particle number fractions associated with polyol-containing spores.
579
580   The Cl1 cluster from WIBS data shows correlations with estimated fungal spores from arabitol
581 and mannitol that have slope much closer to 1.0 than correlations with UV-APS number (Figs. 6g, h,
582 Table S3). For example, the slope of the Cl1 correlations with each polyol during Rainy periods is
583 approximately 0.87. This suggests only a 13% difference between the spore concentration estimates from
584 the two techniques during Rainy periods. The average number concentration of Cl1 during Rainy periods
585 is 1.6×10^4 (± 0.8) spores m^{-3}. In both cases the slopes with respect to Cl1 is greater than 1.0 during Dry
586 periods, suggesting that the cluster method may be missing some fraction of weakly fluorescent particles.
587 Huffman et al. (2012) similarly suggests that that particles that are weakly fluorescent may be below the
588 detection limit of the instrument, and Healy et al. (2014) suggested that both UV-APS and WIBS-4
589 instruments significantly under-count the ubiquitous *Cladosporium* spores that are most common during
590 dry weather and often peak in the afternoon when RH is low (De Groot, 1968; Oliveira et al., 2009).
591 Fundamentally, however, the results from the UV-APS, and even more so the numbers reported by the
592 clustering analysis by Crawford et al. (2015), reveal broadly similar trends with the numbers estimated
593 from polyol-to-spore values reported by Bauer et al. (2008a).
594
595   The fungal culture samples show similar division during Rainy and Dry periods as arabitol and
596 mannitol concentrations (Figure 6c), with an increase of approx. 1.6 during Rainy periods. The trend of a
597 positive slope with respect to the UV-LIF measurements is also similar between the tracer and culturing
598 methods. In general, however, the R^2 value correlating CFU to fungal spore number calculated from UV-
599 LIF number is lower than between tracers and UV-LIF numbers (Table 2). This is not unexpected for
600 several reasons. First, the short sampling time of the culture samples (20 min) leads to poor counting
601 statistics and high number concentration variability, whereas each data point from the high volume air
602 samples represents a period of 4 – 48 hours. Second, culture samplers, by their nature, only account for

culturable fungal spores. It has been estimated that as low as 17% of aerosolized fungal species are culturable, and so it is expected that the CFU concentration observed is significantly less than the total airborne concentration of spores (Bridge and Spooner, 2001; Després et al., 2012). Nonetheless, the culturing analysis here supports the tracer and UV-LIF analyses and the most important trends are consistent between all analysis methods. The concentration of fungal spores is higher during the Rainy periods, and there is a positive correlation between both tracer and CFU concentration and UV-LIF number.

In pristine environment, such as the Amazon, supermicron particle mass has been found to consist of up to 85% biological material (Pöschl et al., 2010). Total particulate matter mass was calculated here from the UV-APS number concentrations (m^{-3}) and converted to mass for particles of aerodynamic diameter 0.5 – 15 μm. In only this case a density of 1.5 g cm^{-3} was utilized to calculate a first approximation of total particle mass to which all other mass measurements were compared. An average TSP mass density of 1.5 g cm^{-3} was utilized, because organic aerosol is typically estimated with density < 1.0 g cm^{-3}, biological particles are often assumed to have ca. 1.0 g cm^{-3} density, and mineral dust particles have densities of up to ca. 3.5 g cm^{-3} (Dexter, 2004; Tegen and Fung, 1994). Fungal spore mass was estimated here using the fungal spore concentrations calculated from arabitol and mannitol mass (Fig. 6) and then using an estimated 33 pg reported by Bauer et al. (2008b) as an average mass per spore. Dividing the resultant fungal spore mass by total particulate mass provides a relative mass fraction for each high volume sample period. These calculations suggest that fungal spores represent approximately 23% ± 9 (using arabitol) or 21% ± 8 (using mannitol) of total particulate mass during Rainy periods (Table 3, Figure 7). This represents a nearly 6 fold increase in percentage compared to Dry periods (4.8% ± 1.4 and 3.7% ± 1.1, respectively). A similar increase during Rainy periods was also seen in the mass fraction of fungal cluster Cl1, which represented 17% ± 10 of the particle mass during Rainy and 2% ± 1 during Dry periods (Table S4).

3.5 Variations in endotoxin and glucan concentrations

Endotoxins measured in the atmosphere are uniquely associated with gram-negative bacteria (Andreae and Crutzen, 1997). Here, we show correlations between total endotoxin mass and WIBS Cl_{Bact}, which was assigned by Crawford et al. (2015) to be bacteria due to the small particle size (< 1 μm) and high correlation with rain. These assignment of particle type to this set of clusters is quite uncertain, however, and should be treated loosely. The correlation between endotoxin mass and UV-APS and the WIBS clusters was very poor, in most cases R^2 <0.1 (Table 2, Figure 8), suggesting no apparent relationship. Analysis of bacteria by both UV-LIF techniques is hampered by the fact that bacteria can be < 1 μm in size and because both instruments detect particles with decreased efficiency at sizes below 0.8 μm. So weak correlations may not have been apparent due to reduced overlap in particle size. Despite the lack of apparent correlation between the techniques, the relatively variable endotoxin concentrations were elevated during Rainy periods, consistent with Jones and Harrison (2004), who showed that bacteria concentration were elevated after rainy periods.

Glucans, such as (1→3)-β-D-glucan, are components of the cell walls of pollen, fungal spores, plant detritus, and bacteria (Chow et al., 2015b; Lee et al., 2006; Stone and Clarke, 1992). In contrast to the observed difference in endotoxin concentration during the different wetness periods, however, (1→3)-β-D-glucan showed no correlations with UV-LIF concentrations (Table 2) and no differentiation during the different wetness periods.

4. Conclusions

Increased concentrations of fluorescent aerosol particles and ice nuclei attributed to having biological origin were observed during and immediately after rain events throughout the BEACHON-RoMBAS study in 2011 (Huffman et al., 2013; Prenni et al., 2013; Schumacher et al., 2013). Here we expand upon the previous reports by utilizing measurements from two commercially available UV-LIF instruments, of several molecular tracers extracted from high volume filter samples, and from a culture-

based sampler in order to compare three very different methods of atmospheric fungal spore analysis. This study represents the first reported correlation of UV-LIF and molecular tracer measurements and provided an opportunity to understand how an important class of PBAP might be influenced by periods of rainy and dry weather. We found clear patterns in the fungal molecular tracers, arabitol and mannitol, associated with Rainy conditions that are consistent with previous findings (Bauer et al., 2008a; Elbert et al., 2007; Feofilova, 2001). Fungal polyols increased 3-fold over Dry conditions during Rainy weather samples, with arabitol concentration of 35.2 ± 10.5 ng m^{-3} and mannitol concentration of 44.9 ± 13.8 ng m^{-3}. Additionally, the very high correlation of the fungal tracers with WIBS Cl1 ($R^2 > 0.8$ in many cases) provides support for its assignment by Crawford et al. (2015) to fungal spores. Similarly, the UV-APS correlates well with fungal tracers, however over-counts the number concentration estimated from the tracers, confirming that the UV-APS is sensitive also to other types of particles beyond fungal spores, as expected. The estimated spore count from the WIBS Cl1 concentration was within ~13% of the spore count estimated by the tracer method, with concentrations ranging from $1.6 – 2.9$ x 10^4 spores m^{-3}. These values are broadly consistent with concentrations modeled by, e.g. Spracklen and Heald (2014), Hoose et al. (2010), and Hummel et al. (2015). These spore counts represent 17-23% of the total particle mass during Rainy conditions and 2-4% during Dry conditions. Culture-based sampling also shows a similar relationship between CFU and UV-LIF concentrations and an increase of ~1.6 between Dry and Rainy conditions. Despite the fact that the tracer and UV-LIF approaches to estimating atmospheric fungal spore concentration are fundamentally different, they provide remarkably similar estimates and temporal trends. With further improvements in instrumentation and analysis methods (e.g. advanced clustering algorithms applied to UV-LIF data), the ability to reliably discriminate between PBAP types is improving. As we have shown here, this technology represents a potential for monitoring approximate fungal spore mass and for contributing improved information on fungal spore concentration to global and regional models that to this point has been lacking (Spracklen and Heald, 2014).

5. Acknowledgements

The BEACHON-RoMBAS campaign was partially supported by an ETBC (Emerging Topics in Biogeochemical Cycles) grant to the National Center for Atmospheric Research (NCAR), the University of Colorado, Colorado State University, and Penn State University (NSF ATM-0919189). The authors wish to thank Jose Jimenez, Douglas Day (Univ. Colorado-Boulder); Anthony Prenni, Paul DeMott, Sonia Kreidenweis, and Jessica Prenni (Colorado St. Univ.); Alex Guenther, and Jim Smith (NCAR) for BEACHON-RoMBAS project organization and logistical support and the USFS, NCAR, and Richard Oakes for access to the Manitou Experimental Forest Observatory field site. Measurements of temperature, relative humidity, wind speed, and wind direction were provided by Andrew Turnipseed (NCAR) and leaf wetness and disdrometer data were provided by Dave Gochis (NCAR). Marie I. Gosselin thanks the Max Planck Society for financial support. J. Alex Huffman thanks the University of Denver for intramural funding for faculty support. The Mainz team acknowledges the Mainz Bioaerosol Laboratory (MBAL) and financial support from the Max Planck Society (MPG), the Max Planck Graduate Center with the Johannes Gutenberg University Mainz (MPGC), the Geocycles Cluster Mainz (LEC Rheinland-Pfalz), and the German Research Foundation (DFG PO1013/5-1 and FR3641/1-2, FOR 1525 INUIT). The Manchester team acknowledges funding from the UK NERC (UK-BEACHON, Grant # NE/H019049/1) to participate in the BEACHON experiment, and development support of the WIBS instruments. Manchester would also like to thank Prof. Paul Kaye, the developer of the WIBS instruments and his team at the University of Hertfordshire, for their technical support. The authors thank Cristina Ruzene, Isabell Müller-Germann, Petya Yordanova, Tobias Könemann (Max Planck Inst. For Chem.), and Nicole Savage (Univ. Denver) for technical assistance.

6. References

Allitt, U.: Airborne fungal spores and the thunderstorm of 24 June 1994, Aerobiologia, 16, 397-406, 2000.

Andreae, M. O. and Crutzen, P. J.: Atmospheric Aerosols: Biogeochemical Sources and Role in Atmospheric Chemistry, Science, 276, 1052-1058, 10.1126/science.276.5315.1052, 1997.

Axelsson, B.-O., Saraf, A., and Larsson, L.: Determination of ergosterol in organic dust by gas chromatography-mass spectrometry, Journal of Chromatography B: Biomedical Sciences and Applications, 666, 77-84, http://dx.doi.org/10.1016/0378-4347(94)00553-H, 1995.

Barbaro, E., Kirchgeorg, T., Zangrando, R., Vecchiato, M., Piazza, R., Barbante, C., and Gambaro, A.: Sugars in Antarctic aerosol, Atmos Environ, 118, 135-144, http://dx.doi.org/10.1016/j.atmosenv.2015.07.047, 2015.

Bauer, H., Claeys, M., Vermeylen, R., Schueller, E., Weinke, G., Berger, A., and Puxbaum, H.: Arabitol and mannitol as tracers for the quantification of airborne fungal spores, Atmos Environ, 42, 588-593, 10.1016/j.atmosenv.2007.10.013, 2008a.

Bauer, H., Schueller, E., Weinke, G., Berger, A., Hitzenberger, R., Marr, I. L., and Puxbaum, H.: Significant contributions of fungal spores to the organic carbon and to the aerosol mass balance of the urban atmospheric aerosol, Atmos Environ, 42, 5542-5549, 10.1016/j.atmosenv.2008.03.019, 2008b.

Bigg, E. K., Soubeyrand, S., and Morris, C. E.: Persistent after-effects of heavy rain on concentrations of ice nuclei and rainfall suggest a biological cause, Atmos Chem Phys, 15, 2313-2326, 2015.

Bridge, P. and Spooner, B.: Soil fungi: diversity and detection, Plant and soil, 232, 147-154, 2001.

Buller, A.: Spore deposits—the number of spores, Researches on fungi, 1, 79-88, 1909.

Burger, H.: Official Publication of American Academy of Allergy and ImmunologyBioaerosols: Prevalence and health effects in the indoor environment, Journal of Allergy and Clinical Immunology, 86, 687-701, http://dx.doi.org/10.1016/S0091-6749(05)80170-8, 1990.

Burshtein, N., Lang-Yona, N., and Rudich, Y.: Ergosterol, arabitol and mannitol as tracers for biogenic aerosols in the eastern Mediterranean, Atmos Chem Phys, 11, 829-839, 10.5194/acp-11-829-2011, 2011.

Caseiro, A., Marr, I. L., Claeys, M., Kasper-Giebl, A., Puxbaum, H., and Pio, C. A.: Determination of saccharides in atmospheric aerosol using anion-exchange high-performance liquid chromatography and pulsed-amperometric detection, Journal of Chromatography A, 1171, 37-45, http://dx.doi.org/10.1016/j.chroma.2007.09.038, 2007.

Cheng, J. Y. W., Hui, E. L. C., and Lau, A. P. S.: Bioactive and total endotoxins in atmospheric aerosols in the Pearl River Delta region, China, Atmos Environ, 47, 3-11, http://dx.doi.org/10.1016/j.atmosenv.2011.11.055, 2012.

Chow, J. C., Lowenthal, D. H., Chen, L.-W. A., Wang, X., and Watson, J. G.: Mass reconstruction methods for PM2. 5: a review, Air Quality, Atmosphere & Health, 8, 243-263, 2015a.

738   Chow, J. C., Yang, X., Wang, X., Kohl, S. D., Hurbain, P. R., Chen, L. A., and Watson, J. G.:
739   Characterization of Ambient PM10 Bioaerosols in a California Agricultural Town, Aerosol Air Qual Res,
740   15, 1433-1447, 2015b.

741   Crawford, I., Robinson, N. H., Flynn, M. J., Foot, V. E., Gallagher, M. W., Huffman, J. A., Stanley, W.
742   R., and Kaye, P. H.: Characterisation of bioaerosol emissions from a Colorado pine forest: results from
743   the BEACHON-RoMBAS experiment, Atmos Chem Phys, 14, 8559-8578, 10.5194/acp-14-8559-2014,
744   2014.

745   Crawford, I., Ruske, S., Topping, D., and Gallagher, M.: Evaluation of hierarchical agglomerative cluster
746   analysis methods for discrimination of primary biological aerosol, Atmos Meas Tech, 8, 4979-4991,
747   2015.

748   Dales, R. E., Cakmak, S., Judek, S., Dann, T., Coates, F., Brook, J. R., and Burnett, R. T.: The role of
749   fungal spores in thunderstorm asthma, Chest, 123, 745-750, 2003.

750   De Groot, R.: Diurnal cycles of air-borne spores produced by forest fungi, Phytopathology, 58, 1223-
751   1229, 1968.

752   Deguillaume, L., Leriche, M., Amato, P., Ariya, P. A., Delort, A. M., Pöschl, U., Chaumerliac, N., Bauer,
753   H., Flossmann, A. I., and Morris, C. E.: Microbiology and atmospheric processes: chemical interactions
754   of primary biological aerosols, Biogeosciences, 5, 1073-1084, 10.5194/bg-5-1073-2008, 2008.

755   Després, V. R., Huffman, J. A., Burrows, S. M., Hoose, C., Safatov, A. S., Buryak, G., Frohlich-
756   Nowoisky, J., Elbert, W., Andreae, M. O., Poschl, U., and Jaenicke, R.: Primary biological aerosol
757   particles in the atmosphere: a review, Tellus B, 64, 58, Artn 15598 10.3402/Tellusb.V64i0.15598, 2012.

758   Dexter, A.: Soil physical quality: Part I. Theory, effects of soil texture, density, and organic matter, and
759   effects on root growth, Geoderma, 120, 201-214, 2004.

760   Di Filippo, P., Pomata, D., Riccardi, C., Buiarelli, F., and Perrino, C.: Fungal contribution to size-
761   segregated aerosol measured through biomarkers, Atmos Environ, 64, 132-140, 2013.

762   Douwes, J., Thorne, P., Pearce, N., and Heederik, D.: Bioaerosol health effects and exposure assessment:
763   progress and prospects, Annals of Occupational Hygiene, 47, 187-200, 2003.

764   Elbert, W., Taylor, P. E., Andreae, M. O., and Poschl, U.: Contribution of fungi to primary biogenic
765   aerosols in the atmosphere: wet and dry discharged spores, carbohydrates, and inorganic ions, Atmos
766   Chem Phys, 7, 4569-4588, 2007.

767   Faulwetter, R.: Wind-blown rain, a factor in disease dissemination, J. agric. Res, 10, 639-648, 1917.

768   Feofilova, E. P.: The Kingdom Fungi: Heterogeneity of Physiological and Biochemical Properties and
769   Relationships with Plants, Animals, and Prokaryotes (Review), Applied Biochemistry and Microbiology,
770   37, 124-137, 10.1023/a:1002863311534, 2001.

771   Foot, V. E., Kaye, P. H., Stanley, W. R., Barrington, S. J., Gallagher, M., and Gabey, A.: Low-cost real-
772   time multiparameter bio-aerosol sensors, 2008, 71160I-71160I-71112.

773   Frankland, A. and Gregory, P.: Allergenic and agricultural implications of airborne ascospore
774   concentrations from a fungus, Didymella exitialis, 1973. 1973.

775   Fröhlich-Nowoisky, J., Burrows, S., Xie, Z., Engling, G., Solomon, P., Fraser, M., Mayol-Bracero, O.,
776   Artaxo, P., Begerow, D., and Conrad, R.: Biogeography in the air: fungal diversity over land and oceans,
777   Biogeosciences, 9, 1125-1136, 2012.

778   Fröhlich-Nowoisky, J., Kampf, C. J., Weber, B., Huffman, J. A., Pöhlker, C., Andreae, M. O., Lang-
779   Yona, N., Burrows, S. M., Gunthe, S. S., Elbert, W., Su, H., Hoor, P., Thines, E., Hoffmann, T., Després,
780   V. R., Pöschl, U.: Bioaerosols in the Earth System: Climate, Health, and Ecosystem Interactions,
781   Atmospheric Research, 182, 346-376, 10.1016/j.atmosres.2016.07.018, 2016.

782   Fröhlich-Nowoisky, J., Pickersgill, D. A., Després, V. R., and Pöschl, U.: High diversity of fungi in air
783   particulate matter, Proceedings of the National Academy of Sciences, 106, 12814-12819, 2009.

784   Gabey, A., Gallagher, M., Whitehead, J., Dorsey, J., Kaye, P. H., and Stanley, W.: Measurements and
785   comparison of primary biological aerosol above and below a tropical forest canopy using a dual channel
786   fluorescence spectrometer, Atmos Chem Phys, 10, 4453-4466, 2010.

787   Gilardoni, S., Vignati, E., Marmer, E., Cavalli, F., Belis, C., Gianelle, V., Loureiro, A., and Artaxo, P.:
788   Sources of carbonaceous aerosol in the Amazon basin, Atmos Chem Phys, 11, 2747-2764, 2011.

789   Gonçalves, F. L. T., Bauer, H., Cardoso, M. R. A., Pukinskas, S., Matos, D., Melhem, M., and Puxbaum,
790   H.: Indoor and outdoor atmospheric fungal spores in the São Paulo metropolitan area (Brazil): species and
791   numeric concentrations, International journal of biometeorology, 54, 347-355, 2010.

792   Graham, B., Guyon, P., Taylor, P. E., Artaxo, P., Maenhaut, W., Glovsky, M. M., Flagan, R. C., and
793   Andreae, M. O.: Organic compounds present in the natural Amazonian aerosol: Characterization by gas
794   chromatography-mass spectrometry, J Geophys Res-Atmos, 108, 4766-4766, 10.1029/2003jd003990,
795   2003.

796   Gregory, P. H. and Sreeramulu, T.: Air spora of an estuary, T Brit Mycol Soc, 41, 145-156,
797   http://dx.doi.org/10.1016/S0007-1536(58)80025-X, 1958.

798   Haga, D., Iannone, R., Wheeler, M., Mason, R., Polishchuk, E., Fetch, T., Kamp, B., McKendry, I., and
799   Bertram, A.: Ice nucleation properties of rust and bunt fungal spores and their transport to high altitudes,
800   where they can cause heterogeneous freezing, Journal of Geophysical Research: Atmospheres, 118, 7260-
801   7272, 2013.

802   Hairston, P. P., Ho, J., and Quant, F. R.: Design of an instrument for real-time detection of bioaerosols
803   using simultaneous measurement of particle aerodynamic size and intrinsic fluorescence, Journal of
804   Aerosol Science, 28, 471-482, 1997.

805   Heald, C. L. and Spracklen, D. V.: Atmospheric budget of primary biological aerosol particles from
806   fungal spores, Geophysical Research Letters, 36, L09806/09801-L09806/09805, 2009.

807   Healy, D., Huffman, J., O'Connor, D., Pöhlker, C., Pöschl, U., and Sodeau, J.: Ambient measurements of
808   biological aerosol particles near Killarney, Ireland: a comparison between real-time fluorescence and
809   microscopy techniques, Atmos Chem Phys, 14, 8055-8069, 2014.

810   Hernandez, M., Perring, A. E., McCabe, K., Kok, G., Granger, G., and Baumgardner, D.: Chamber
811   catalogues of optical and fluorescent signatures distinguish bioaerosol classes, Atmos Meas Tech, 9,
812   3283-3292, 2016.

813 Hill, S. C., Mayo, M. W., and Chang, R. K.: Fluorescence of bacteria, pollens, and naturally occurring
814 airborne particles: excitation/emission spectra, DTIC Document, 2009.

815 Hill, S. C., Pan, Y.-L., Williamson, C., Santarpia, J. L., and Hill, H. H.: Fluorescence of bioaerosols:
816 mathematical model including primary fluorescing and absorbing molecules in bacteria, Optics Express,
817 21, 22285-22313, 10.1364/oe.21.022285, 2013.

818 Hill, S. C., Williamson, C. C., Doughty, D. C., Pan, Y.-L., Santarpia, J. L., and Hill, H. H.: Size-
819 dependent fluorescence of bioaerosols: Mathematical model using fluorescing and absorbing molecules in
820 bacteria, Journal of Quantitative Spectroscopy and Radiative Transfer, 157, 54-70,
821 http://dx.doi.org/10.1016/j.jqsrt.2015.01.011, 2015.

822 Hirst, J. and Stedman, O.: Dry liberation of fungus spores by raindrops, Microbiology, 33, 335-344, 1963.

823 Hoose, C., Kristjánsson, J. E., Chen, J.-P., and Hazra, A.: A Classical-Theory-Based Parameterization of
824 Heterogeneous Ice Nucleation by Mineral Dust, Soot, and Biological Particles in a Global Climate Model,
825 Journal of the Atmospheric Sciences, 67, 2483-2503, doi:10.1175/2010JAS3425.1, 2010.

826 Huffman, J. A., Prenni, A. J., DeMott, P. J., Pöhlker, C., Mason, R. H., Robinson, N. H., Fröhlich-
827 Nowoisky, J., Tobo, Y., Després, V. R., Garcia, E., Gochis, D. J., Harris, E., Müller-Germann, I., Ruzene,
828 C., Schmer, B., Sinha, B., Day, D. A., Andreae, M. O., Jimenez, J. L., Gallagher, M., Kreidenweis, S. M.,
829 Bertram, A. K., and Pöschl, U.: High concentrations of biological aerosol particles and ice nuclei during
830 and after rain, Atmos. Chem. Phys., 13, 6151-6164, 10.5194/acp-13-6151-2013, 2013.

831 Huffman, J. A. and Santarpia, J.: Online techniques for quantification and characterization of biological
832 aerosol. In: Microbiology of aerosols, Delort, A.-M. and Amato, P., Wiley, Hoboken, NJ, In Press, 2016.

833 Huffman, J. A., Sinha, B., Garland, R. M., Snee-Pollmann, A., Gunthe, S. S., Artaxo, P., Martin, S. T.,
834 Andreae, M. O., and Pöschl, U.: Size distributions and temporal variations of biological aerosol particles
835 in the Amazon rainforest characterized by microscopy and real-time UV-APS fluorescence techniques
836 during AMAZE-08, Atmos. Chem. Phys., 12, 11997-12019, 10.5194/acp-12-11997-2012, 2012.

837 Hummel, M., Hoose, C., Gallagher, M., Healy, D. A., Huffman, J. A., O'Connor, D., Poeschl, U.,
838 Poehlker, C., Robinson, N. H., Schnaiter, M., Sodeau, J. R., Stengel, M., Toprak, E., and Vogel, H.:
839 Regional-scale simulations of fungal spore aerosols using an emission parameterization adapted to local
840 measurements of fluorescent biological aerosol particles, Atmos Chem Phys, 15, 6127-6146, 2015.

841 Ingold, C. T.: Fungal spores: Their liberation and dispersal. 1971.

842 Jones, A. M. and Harrison, R. M.: The effects of meteorological factors on atmospheric bioaerosol
843 concentrations—a review, Science of the Total Environment, 326, 151-180,
844 http://dx.doi.org/10.1016/j.scitotenv.2003.11.021, 2004.

845 Kaye, P., Stanley, W., Hirst, E., Foot, E., Baxter, K., and Barrington, S.: Single particle multichannel bio-
846 aerosol fluorescence sensor, Optics Express, 13, 3583-3593, 2005.

847 Lau, A. P. S., Lee, A. K. Y., Chan, C. K., and Fang, M.: Ergosterol as a biomarker for the quantification
848 of the fungal biomass in atmospheric aerosols, Atmos Environ, 40, 249-259, 2006.

849 Laumbach, R. J. and Kipen, H. M.: Bioaerosols and sick building syndrome: particles, inflammation, and
850 allergy, Current opinion in allergy and clinical immunology, 5, 135-139, 2005.

851 Lee, T., Grinshpun, S. A., Kim, K. Y., Iossifova, Y., Adhikari, A., and Reponen, T.: Relationship between
852 indoor and outdoor airborne fungal spores, pollen, and $(1\rightarrow 3)$-β-D-glucan in homes without visible mold
853 growth, Aerobiologia, 22, 227-235, 2006.

854 Lee, T., Sullivan, A. P., Mack, L., Jimenez, J. L., Kreidenweis, S. M., Onasch, T. B., Worsnop, D. R.,
855 Malm, W., Wold, C. E., Hao, W. M., and Collett, J. L., Jr.: Chemical Smoke Marker Emissions During
856 Flaming and Smoldering Phases of Laboratory Open Burning of Wildland Fuels, Aerosol Science and
857 Technology, 44, I-V, 2010.

858 Lewis, D. H. and Smith, D. C.: Sugar alcohols (polyols) in fungi and green plants, New Phytol, 66, 185-
859 204, 1967.

860 Liang, L., Engling, G., He, K., Du, Z., Cheng, Y., and Duan, F.: Evaluation of fungal spore characteristics
861 in Beijing, China, based on molecular tracer measurements, Environmental Research Letters, 8, 014005,
862 2013.

863 Lin, W.-H. and Li, C.-S.: Associations of fungal aerosols, air pollutants, and meteorological factors,
864 Aerosol Science & Technology, 32, 359-368, 2000.

865 Linneberg, A.: The increase in allergy and extended challenges, Allergy, 66, 1-3, 2011.

866 Madden, L.: Effects of rain on splash dispersal of fungal pathogens, Canadian Journal of Plant Pathology,
867 19, 225-230, 1997.

868 Madelin, T.: Fungal aerosols: a review, Journal of Aerosol Science, 25, 1405-1412, 1994.

869 Miller, J. D. and Young, J. C.: The use of ergosterol to measure exposure to fungal propagules in indoor
870 air, American Industrial Hygiene Association Journal, 58, 39-43, 1997.

871 Morris, C., Sands, D., Glaux, C., Samsatly, J., Asaad, S., Moukahel, A., Goncalves, F. L. T., and Bigg, E.:
872 Urediospores of rust fungi are ice nucleation active at$>-$ 10 C and harbor ice nucleation active bacteria,
873 Atmos Chem Phys, 13, 4223-4233, 2013.

874 Oliveira, M., Ribeiro, H., Delgado, J., and Abreu, I.: The effects of meteorological factors on airborne
875 fungal spore concentration in two areas differing in urbanisation level, International journal of
876 biometeorology, 53, 61-73, 2009.

877 Ortega, J., Turnipseed, A., Guenther, A. B., Karl, T. G., Day, D. A., Gochis, D., Huffman, J. A., Prenni,
878 A. J., Levin, E. J. T., Kreidenweis, S. M., DeMott, P. J., Tobo, Y., Patton, E. G., Hodzic, A., Cui, Y. Y.,
879 Harley, P. C., Hornbrook, R. S., Apel, E. C., Monson, R. K., Eller, A. S. D., Greenberg, J. P., Barth, M.
880 C., Campuzano-Jost, P., Palm, B. B., Jimenez, J. L., Aiken, A. C., Dubey, M. K., Geron, C., Offenberg,
881 J., Ryan, M. G., Fornwalt, P. J., Pryor, S. C., Keutsch, F. N., DiGangi, J. P., Chan, A. W. H., Goldstein,
882 A. H., Wolfe, G. M., Kim, S., Kaser, L., Schnitzhofer, R., Hansel, A., Cantrell, C. A., Mauldin, R. L., and
883 Smith, J. N.: Overview of the Manitou Experimental Forest Observatory: site description and selected
884 science results from 2008 to 2013, Atmos Chem Phys, 14, 6345-6367, 10.5194/acp-14-6345-2014, 2014.

885 Perring, A., Schwarz, J., Baumgardner, D., Hernandez, M., Spracklen, D., Heald, C., Gao, R., Kok, G.,
886 McMeeking, G., and McQuaid, J.: Airborne observations of regional variation in fluorescent aerosol
887 across the United States, Journal of Geophysical Research: Atmospheres, 120, 1153-1170, 2015.

888 Pohlker, C., Huffman, J. A., Forster, J. D., and Poschl, U.: Autofluorescence of atmospheric bioaerosols:
889 spectral fingerprints and taxonomic trends of pollen, Atmos Meas Tech, 6, 3369-3392, 10.5194/amt-6-
890 3369-2013, 2013.

891 Pöhlker, C., Huffman, J. A., and Poeschl, U.: Autofluorescence of atmospheric bioaerosols-fluorescent
892 biomolecules and potential interferences, Atmos Meas Tech, 5, 37-71, 2012a.

893 Pöhlker, C., Wiedemann, K. T., Sinha, B., Shiraiwa, M., Gunthe, S. S., Smith, M., Su, H., Artaxo, P.,
894 Chen, Q., and Cheng, Y.: Biogenic potassium salt particles as seeds for secondary organic aerosol in the
895 Amazon, Science, 337, 1075-1078, 2012b.

896 Pöschl, U., Martin, S., Sinha, B., Chen, Q., Gunthe, S., Huffman, J., Borrmann, S., Farmer, D., Garland,
897 R., and Helas, G.: Rainforest aerosols as biogenic nuclei of clouds and precipitation in the Amazon,
898 Science, 329, 1513-1516, 2010.

899 Pöschl, U. and Shiraiwa, M.: Multiphase chemistry at the atmosphere–biosphere interface influencing
900 climate and public health in the Anthropocene, Chemical reviews, 115, 4440-4475, 2015.

901 Prenni, A. J., Tobo, Y., Garcia, E., DeMott, P. J., Huffman, J. A., McCluskey, C. S., Kreidenweis, S. M.,
902 Prenni, J. E., Pöhlker, C., and Pöschl, U.: The impact of rain on ice nuclei populations at a forested site in
903 Colorado, Geophysical Research Letters, 40, 227-231, 10.1029/2012gl053953, 2013.

904 Pyrri, I. and Kapsanaki-Gotsi, E.: A comparative study on the airborne fungi in Athens, Greece, by viable
905 and non-viable sampling methods, Aerobiologia, 23, 3-15, 2007.

906 Rasband, W. and ImageJ, U.: Bethesda, Md, USA. ImageJ, 1997.

907 Rathnayake, C. M., Metwali, N., Baker, Z., Jayarathne, T., Kostle, P. A., Thorne, P. S., O'Shaughnessy, P.
908 T., and Stone, E. A.: Urban enhancement of PM10 bioaerosol tracers relative to background locations in
909 the Midwestern United States, Journal of Geophysical Research: Atmospheres, 121, 5071-5089, 2016a.

910 Rathnayake, C. M., Metwali, N., Jayarathne, T., Kettler, J., Huang, Y., Thorne, P. S., O'Shaughnessy, P.
911 T., and Stone, E. A.: Influence of Rain on the Abundance and Size Distribution of Bioaerosols, Atmos.
912 Chem. Phys. Discuss., 2016, 1-29, 10.5194/acp-2016-622, 2016b.

913 Robinson, N. H., Allan, J. D., Huffman, J. A., Kaye, P. H., Foot, V. E., and Gallagher, M.: Cluster
914 analysis of WIBS single-particle bioaerosol data, Atmos Meas Tech, 6, 337-347, 10.5194/amt-6-337-
915 2013, 2013.

916 Ruske, S., Topping, D. O., Foot, V. E., Kaye, P. H., Stanley, W. R., Crawford, I., Morse, A. P., and
917 Gallagher, M. W.: Evaluation of Machine Learning Algorithms for Classification of Primary Biological
918 Aerosol using a new UV-LIF spectrometer, 2016. 2016.

919 Saari, S., Niemi, J., Rönkkö, T., Kuuluvainen, H., Järvinen, A., Pirjola, L., Aurela, M., Hillamo, R., and
920 Keskinen, J.: Seasonal and diurnal variations of fluorescent bioaerosol concentration and size distribution
921 in the urban environment, Aerosol and Air Quality Research, 15, 572-581, 2015.

922 Saari, S., Putkiranta, M., and Keskinen, J.: Fluorescence spectroscopy of atmospherically relevant
923 bacterial and fungal spores and potential interferences, Atmos Environ, 71, 202-209, 2013.

924 Schauer, J. J., Rogge, W. F., Hildemann, L. M., Mazurek, M. A., Cass, G. R., and Simoneit, B. R. T.:
925 Source apportionment of airborne particulate matter using organic compounds as tracers, Atmos Environ,
926 30, 3837-3855, http://dx.doi.org/10.1016/1352-2310(96)00085-4, 1996.

927 Schumacher, C. J., Pöhlker, C., Aalto, P., Hiltunen, V., Petäjä, T., Kulmala, M., Pöschl, U., and Huffman,
928 J. A.: Seasonal cycles of fluorescent biological aerosol particles in boreal and semi-arid forests of Finland
929 and Colorado, Atmos. Chem. Phys., 13, 11987-12001, 10.5194/acp-13-11987-2013, 2013.

930 Sesartic, A. and Dallafior, T. N.: Global fungal spore emissions, review and synthesis of literature data,
931 Biogeosciences, 8, 1181-1192, 10.5194/bg-8-1181-2011, 2011.

932 Sesartic, A., Lohmann, U., and Storelvmo, T.: Modelling the impact of fungal spore ice nuclei on clouds
933 and precipitation, Environmental Research Letters, 8, 014029, 2013.

934 Simoneit, B. R. and Mazurek, M.: Organic tracers in ambient aerosols and rain, Aerosol Science and
935 Technology, 10, 267-291, 1989.

936 Simoneit, B. R. T., Kobayashi, M., Mochida, M., Kawamura, K., Lee, M., Lim, H.-J., Turpin, B. J., and
937 Komazaki, Y.: Composition and major sources of organic compounds of aerosol particulate matter
938 sampled during the ACE-Asia campaign, Journal of Geophysical Research, [Atmospheres], 109,
939 D19S10/11-D19S10/22, 2004.

940 Sodeau, J. and O'Connor, D.: Bioaerosol Monitoring of the Atmosphere for Occupational and
941 Environmental Purposes, Comprehensive Analytical Chemistry, 2016. 2016.

942 Spracklen, D. and Heald, C. L.: The contribution of fungal spores and bacteria to regional and global
943 aerosol number and ice nucleation immersion freezing rates, Atmos Chem Phys, 14, 9051-9059, 2014.

944 Stone, B. and Clarke, A.: Chemistry and biology of (1, 3)-D-glucans, Victoria, Australia.: La Trobe
945 University Press, 1992. 236-239, 1992.

946 Taylor, P. E. and Jonsson, H.: Thunderstorm asthma, Current allergy and asthma reports, 4, 409-413,
947 2004.

948 Tegen, I. and Fung, I.: Modeling of mineral dust in the atmosphere: Sources, transport, and optical
949 thickness, Journal of Geophysical Research: Atmospheres, 99, 22897-22914, 1994.

950 Tobo, Y., Prenni, A. J., DeMott, P. J., Huffman, J. A., McCluskey, C. S., Tian, G., Pöhlker, C., Pöschl,
951 U., and Kreidenweis, S. M.: Biological aerosol particles as a key determinant of ice nuclei populations in
952 a forest ecosystem, Journal of Geophysical Research: Atmospheres, 118, 10,100-110,110,
953 10.1002/jgrd.50801, 2013.

954 Toprak, E. and Schnaiter, M.: Fluorescent biological aerosol particles measured with the Waveband
955 Integrated Bioaerosol Sensor WIBS-4: laboratory tests combined with a one year field study, Atmos.
956 Chem. Phys, 13, 225-243, 2013.

957 Weete, J. D.: Sterols of the fungi: distribution and biosynthesis, Phytochemistry, 12, 1843-1864, 1973.

958 Womiloju, T. O., Miller, J. D., Mayer, P. M., and Brook, J. R.: Methods to determine the biological
959 composition of particulate matter collected from outdoor air, Atmos Environ, 37, 4335-4344, 2003.

960   Yang, Y., Chan, C.-y., Tao, J., Lin, M., Engling, G., Zhang, Z., Zhang, T., and Su, L.: Observation of
961   elevated fungal tracers due to biomass burning in the Sichuan Basin at Chengdu City, China, Science of
962   the Total Environment, 431, 68-77, 2012.

963   Yttri, K. E., Simpson, D., Noejgaard, J. K., Kristensen, K., Genberg, J., Stenstrom, K., Swietlicki, E.,
964   Hillamo, R., Aurela, M., Bauer, H., Offenberg, J. H., Jaoui, M., Dye, C., Eckhardt, S., Burkhart, J. F.,
965   Stohl, A., and Glasius, M.: Source apportionment of the summer time carbonaceous aerosol at Nordic
966   rural background sites, Atmos Chem Phys, 11, 13339-13357, 2011a.

967   Yttri, K. E., Simpson, D., Stenstrom, K., Puxbaum, H., and Svendby, T.: Source apportionment of the
968   carbonaceous aerosol in Norway - quantitative estimates based on 14C, thermal-optical and organic tracer
969   analysis, Atmos Chem Phys, 11, 9375-9394, 2011b.

970   Yue, S., Ren, H., Fan, S., Sun, Y., Wang, Z., and Fu, P.: Springtime precipitation effects on the
971   abundance of fluorescent biological aerosol particles and HULIS in Beijing, Scientific Reports, 6, 2016.

972   Zhang, T., Engling, G., Chan, C.-Y., Zhang, Y.-N., Zhang, Z.-S., Lin, M., Sang, X.-F., Li, Y. D., and Li,
973   Y.-S.: Contribution of fungal spores to particulate matter in a tropical rainforest, Environmental Research
974   Letters, 5, No pp. given, 2010.

975   Zhang, Z., Engling, G., Zhang, L., Kawamura, K., Yang, Y., Tao, J., Zhang, R., Chan, C.-y., and Li, Y.:
976   Significant influence of fungi on coarse carbonaceous and potassium aerosols in a tropical rainforest,
977   Environmental Research Letters, 10, 1-9, 2015.

978   Zhu, C., Kawamura, K., and Kunwar, B.: Organic tracers of primary biological aerosol particles at
979   subtropical Okinawa Island in the western North Pacific Rim, Journal of Geophysical Research:
980   Atmospheres, 120, 5504-5523, 10.1002/2015jd023611, 2015.

981

982

983

Tables and Figures:

985

			Mass Concentration					
			Arabitol (ng m^{-3})		Mannitol (ng m^{-3})		(1→3)-β-D-glucan (pg m^{-3})	
			Rainy	Dry	Rainy	Dry	Rainy	Dry
Mass Concentration	Mannitol (ng m^{-3})	Rainy	**0.839**					
		Dry		0.312				
	(1→3)-β-D-glucan (pg m^{-3})	Rainy	0.000		0.003			
		Dry		0.000		0.327		
	Endotoxins (EU m^{-3})	Rainy	0.116		0.126		**0.427**	
		Dry		0.012		0.113		0.103

986

Table 1: Square of correlation coefficients (R^2) comparing total mass concentration of molecular tracers to each other. EU: endotoxin units. Boxes colored by coefficient value (**Bold Underline**> 0.7; 0.7 > **Bold** > 0.4).

		Mass Concentration								Fungal Spore Number Concentration					
		Arabitol (ng m3)		Mannitol (ng m-3)		(1→3)-β-D-glucan (pg m-3)		Endotoxins (EU m-3)		Arabitol (spores m-3)		Mannitol (spores m-3)		Colony Forming Units (CFU m-3)	
		Rainy	Dry	Rainy	Dry	Rainy	Dry	Rainy	Dry	Rainy	Dry	Rainy	Dry	Rainy	Dry
UVAPS		**_0.732_**	0.127	**_0.877_**	0.160	0.006	0.012	0.153	0.067	**0.483**	0.278	**0.504**	**0.571**	**0.469**	**0.491**
WIBS	FL	**0.554**	0.250	**_0.810_**	0.255	0.128	0.010	0.068	0.066	0.159	0.200	0.088	0.314	0.330	**_0.737_**
	FL1	**0.602**	**0.445**	**_0.819_**	**0.412**	0.042	0.001	0.090	0.012	**0.667**	0.339	**_0.863_**	**0.621**	**0.470**	**0.546**
	FL2	**0.617**	0.248	**_0.843_**	0.342	0.092	0.001	0.039	0.094	**0.485**	0.302	**0.442**	0.340	**0.560**	**0.543**
	FL3	**0.561**	0.222	**_0.818_**	0.251	0.124	0.008	0.071	0.065	0.178	0.181	0.104	0.306	0.367	**_0.736_**
	Cl1	**_0.824_**	**_0.764_**	**_0.799_**	0.109	0.000	0.134	0.229	0.011	**0.679**	**0.543**	**_0.775_**	**0.423**	0.128	**0.690**
	Cl2	0.005	0.002	0.004	0.006	0.002	0.047	0.006	0.017	0.052	0.056	0.001	0.075	0.081	**_0.930_**
	Cl3	0.267	0.164	0.261	0.198	0.003	0.011	0.016	0.066	0.052	0.116	0.087	**0.439**	0.262	0.383
	Cl4	0.048	0.046	0.172	0.118	0.115	0.011	0.179	0.145	0.062	0.089	0.001	0.065	0.120	0.000
	ClBact							0.041	0.081						

Table 2: Square of correlation coefficients (R^2) comparing fluorescent particle measurements from UV-LIF instruments to measurements from molecular tracers and direct-to-agar sampler. Columns marking tracer mass (top line) indicate correlations between time-averaged UV-LIF and tracer mass concentrations (left side), and columns marking fungal spore number indicate correlations between fungal spore number concentrations estimated from time-averaged UV-LIF and tracer or culture measurements (right side). FL1, FL2, FL3 represent individual channels from the WIBS. FL represents particles exhibiting fluorescence in any channel. Cl1, Cl2, Cl3, Cl4 are clusters that estimate particle concentrations as a mixture of various channels (Crawford et al., 2015). Cl$_{Bact}$ is a sum of the "bacteria" clusters Cl2-4. Boxes colored by coefficient value (**Bold Underline** > 0.7; 0.7 > **Bold** > 0.4).

	Mass Concentration						
	Arabitol (ng m^{-3})	Mannitol (ng m^{-3})	Erythritol (ng m^{-3})	Levoglucosan (ng m^{-3})	Glucose (ng m^{-3})	Endotoxins (EU m^{-3})	(1→3)-β-D-glucan (pg m^{-3})
Dry	10.6 ± 2.5 n = 18	11.9 ± 3.2 n=18	0.840 ± 0.610 n=16	14.2 ± 10.7 n=15	38.7 ± 21.3 n=18	0.192 ± 0.0970 n=18	8.85 ± 7.68 n=18
Rainy	35.2 ± 10.5 n=11	44.9 ± 13.8 n=11	1.12 ± 0.38 n=3	12.4 ± 19.1 n=8	73.2 ± 50.5 n=11	1.43 ± 1.22 n=10	10.6 ± 8.2 n=11
Other	20.2 ± 8.9 n=6	22.7 ± 8.3 n=6	0.664 ± 0.515 n=6	9.21 ± 1.66 n=5	56.5 ± 39.2 n=6	0.311 ± 0.159 n=6	6.08 ± 6.08 n=6
	Mass Contribution (%)						
Dry	0.18 % ± 0.05 n=18	0.20 % ± 0.073 n=18	0.014 % ± 0.011 n=16	0.21 % ±0.17 n=15	0.67 % ±0.49 n=18		0.16 % ±0.16 n=18
Rainy	0.83 % ± 0.32 n=11	1.07 % ±0.44 n=11	0.032 % ±0.009 n=3	0.27 % ±0.41 n=8	1.60 % ±1.09 n=11		0.25 % ±0.21 n=11
Other	0.25 % ± 0.28 n=6	0.37 % ± 0.29 n=6	0.013 % ±0.015 n=6	0.15 % ±0.11 n=5	0.83 % ±0.64 n=6		0.12 % ±0.19 n=6
	Fungal Spore Number Concentration (m^{-3})						
Dry	8900 ± 2100 n=18	6900 ± 1900 n=18					

Rainy	29300 ± 8700 n=11	26400 ± 8100 n=11					
Other	16900 ± 7400 n=6	13400 ± 4900 n=6					
	Fungal Spore Mass Contribution (%)						
Dry	4.8 % ± 1.43 n=18	3.7 % ± 1.1 n=18					
Rainy	22.9 % ±8.8 n=11	20.7 % ±8.5 n=11					
Other	9.8 % ± 7.7 n=6	7.3 % ± 5.6 n=6					

Table 3: Campaign-average concentrations of molecular tracers (measured) and fungal spores (number concentration estimated from arabitol and mannitol mass). Each set of data broken into wetness categories. Values are mean ± standard deviation; *n* shows the number of samples used for averaging. Fungal spore mass contribution was based on the assumption by Bauer et al. (2008b) of 33 pg spore[-1]. Total particulate matter mass calculated from UV-APS number concentration (m^{-3}) and converted to mass over aerodynamic particle diameter range 0.5 – 15 μm using density of 1.5 g cm^{-3}.

1004
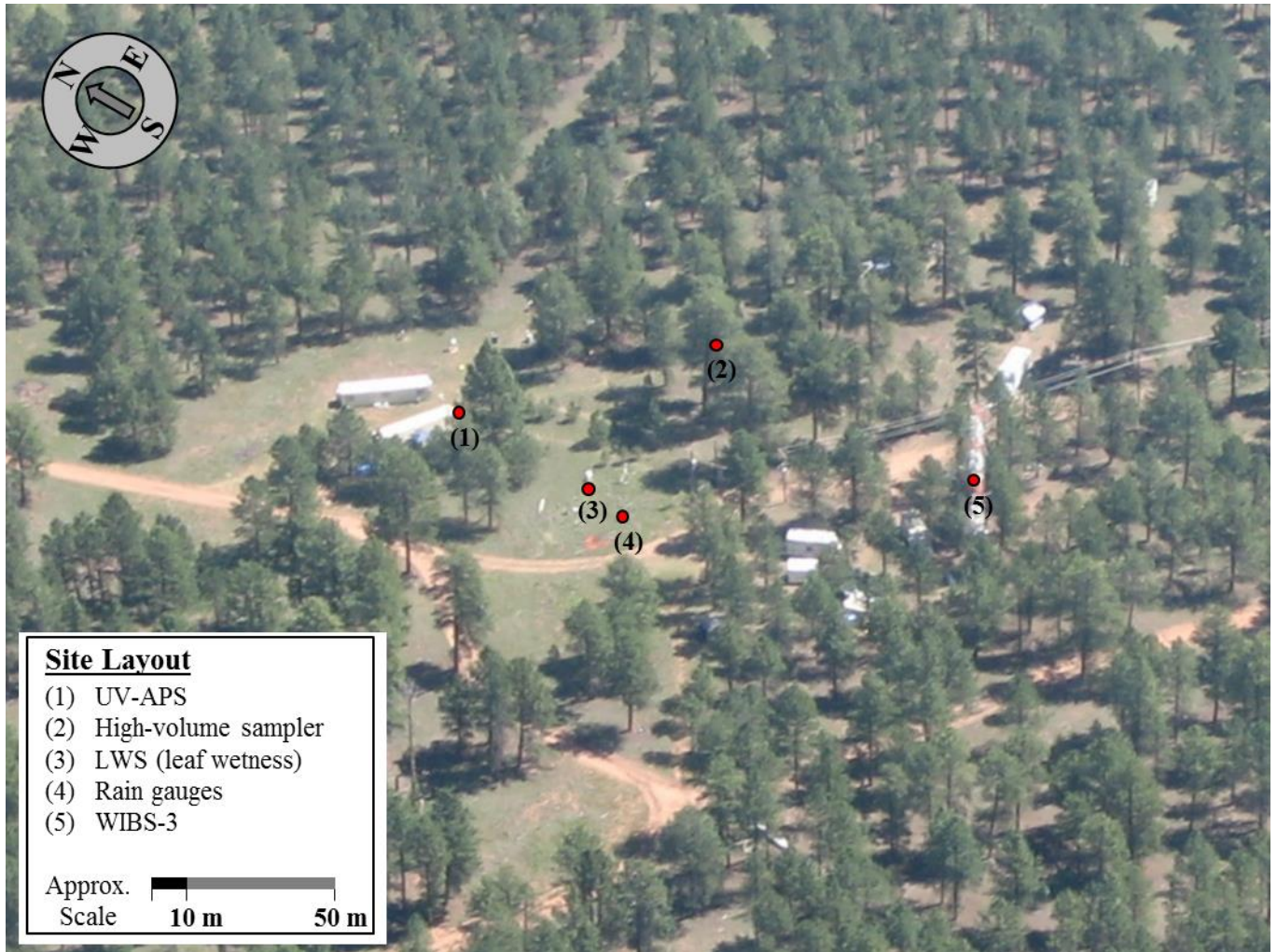
1005
1006
1007 **Figure 1:** Aerial overview of BEACHON-RoMBAS field site at the Manitou Experimental Forest
1008 Observatory located northwest of Colorado Springs, CO. Locations of all instruments and sensors
1009 discussed here are marked and were located within a 50 m radius. Figure adapted from Figure 1a of
1010 Huffman et al. (2013)
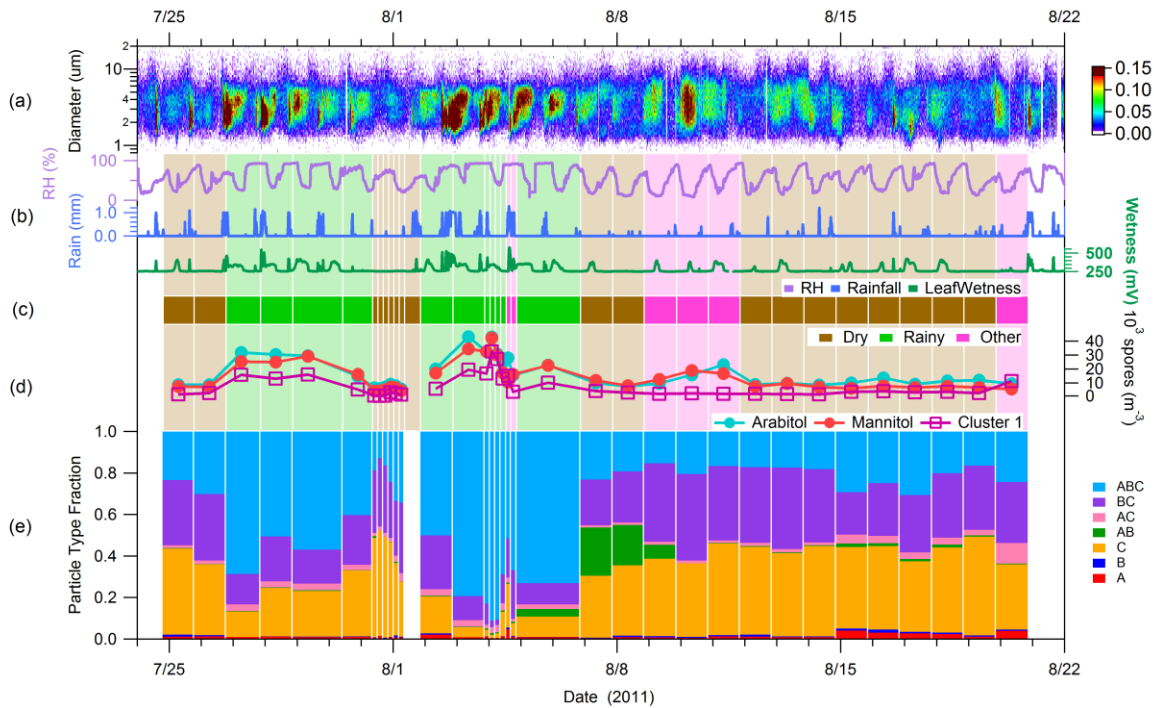
1011
1012 **Figure 2**: Time series of key species concentrations and meteorological data over entire campaign. (a)
1013 Fluorescent particle number size distribution measured with UV-APS instrument. Color scale indicates
1014 fluorescent particle number concentration (L^{-1}). (b) Meteorological data: relative humidity (RH),
1015 disdrometer rainfall (mm per 15 min), leaf wetness (mV). (c) Wetness category indicated as colored bars;
1016 green, Rainy; brown, Dry; pink, Other. Bar width corresponds to filter sampling periods. Lightened
1017 colored bars extend vertically to highlight categorization. (d) Colored traces show fungal spore
1018 concentrations estimated from molecular tracers (circles) and WIBS Cl1 data (squares). (e) Stacked bars
1019 show relative fraction of fluorescent particle type corresponding to each WIBS category.
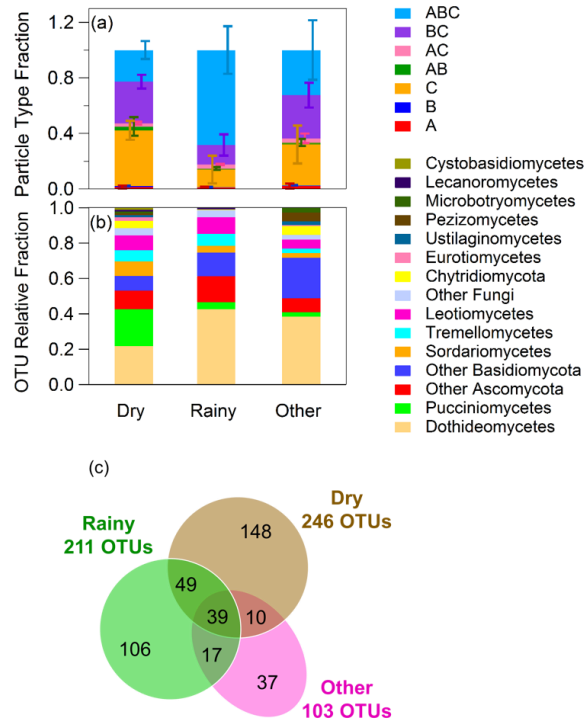
1020
1021 **Figure 3:** Characteristic differences between different wetness periods (Dry, Rainy, Other). (a) Relative
1022 fraction of fluorescent particle number corresponding to each WIBS category. Bars show relative standard
1023 deviation of category fraction in each wetness group (Dry, 19 samples; Rainy, 11 samples; Other, 6
1024 samples). (b, c) Distribution of fungal OTU (operational taxonomic unit) values. (b) Fungal community
1025 composition at phylum and class level with *Agaricomycetes* (dominant class with consistently ~60% of
1026 diversity) removed. Relative proportion of OTUs assigned to different fungal classes and phyla for each
1027 sample category shown. (c) Venn diagram showing the number of unique (wetness category specific) and
1028 shared OTUs (represented by numbers in overlapping areas) among the sample categories (Dry, 11
1029 samples; Rainy, 7 samples; Other, 3 samples). OTUs classified as cluster of sequences with ≥ 97%
1030 similarity. Taxonomic assignments were performed using BLAST against NCBI database. In total, 3902
1031 sequences, representing 406 fungal OTUs from 3 phyla and 12 classes were detected. Despite differences
1032 in community structure across the sample categories, phylogenetic representation appears largely similar.
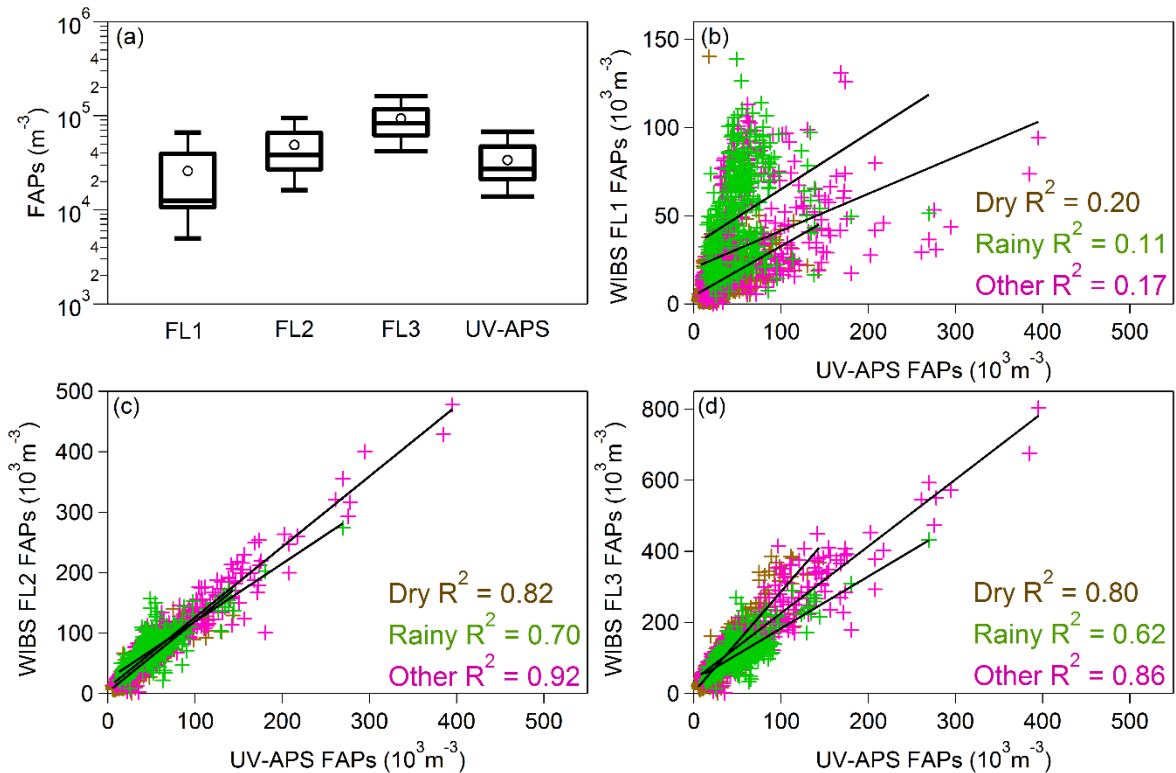
1033
1034 **Figure 4**: Number concentration of fluorescent particles as a function of instrument channel, averaged
1035 over entire measurement period. (a) Box-whisker plot of fluorescent particle number concentration for
1036 WIBS FL1, FL2, FL3, and UVAPS. Circle markers shows mean values, internal horizontal line shows
1037 median, top and bottom of box show inner quartile, and whiskers show 5th and 95th percentiles. (b) WIBS
1038 FL1 versus UV-APS (c) WIBS FL2 versus UV-APS (d) WIBS FL3 versus UV-APS. Crosses represent 5-
1039 minute average points. Linear fits assigned for data in each wetness category.
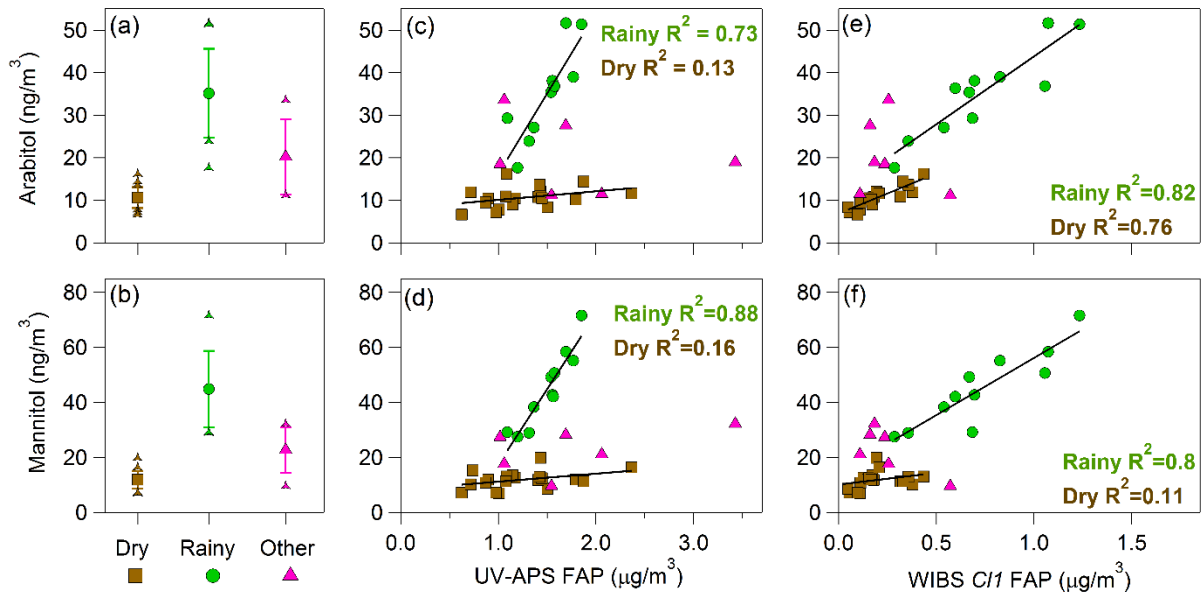
1040
1041

Figure 5: Mass concentrations of molecular tracers and fluorescent particles (assuming unit density particle mass and spherical particles): arabitol – top row, and mannitol – bottom row. Average mass concentration of arabitol (a) and mannitol (b) in each wetness category. Central marker shows mean value of individual filter concentration values, bars represent standard deviation (*s*) range of filter values, and individual points show outliers beyond mean ± *s*. Correlation of arabitol (c) and mannitol (d) with fluorescent particle mass from UV-APS. Correlation of arabitol (e) and mannitol (f) with fluorescent particle mass from WIBS Cluster 1. R^2 values shown for each fit in c-f. Linear fit parameters are shown in Table S2.
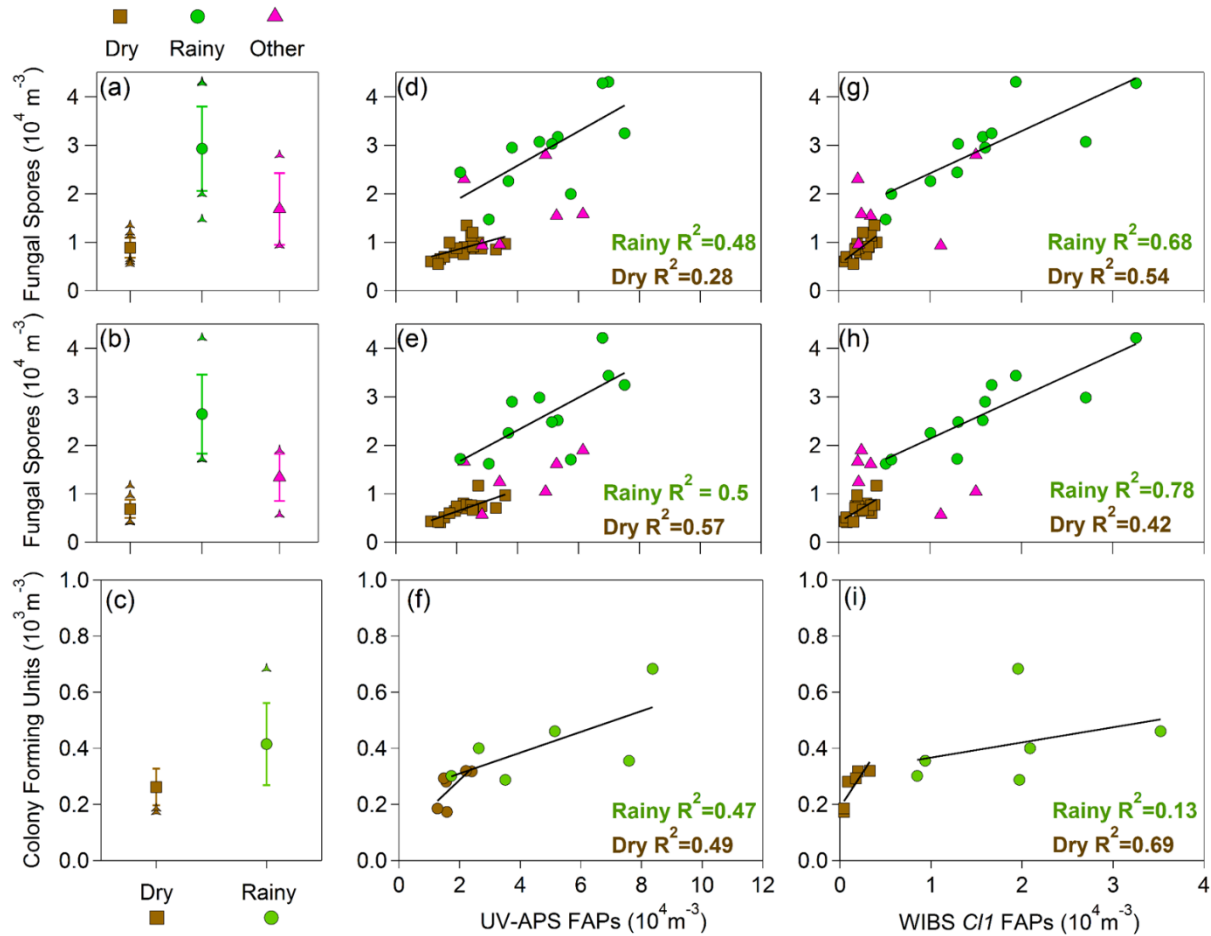
Figure 6: Estimated fungal spore number concentration, calculated using mass of arabitol and mannitol per spore reported by Bauer et al. (2008a). Estimates from arabitol (top row) and mannitol (bottom row). Average fungal spore concentration, calculated using arabitol mass (a), mannitol mass (b), and colony forming units (c) in each wetness category. Central marker shows mean value of individual filter concentration values, bars represent standard deviation (*s*) range of filter values, and individual points show outliers beyond mean ± *s*. Correlation of fungal spore number calculated from arabitol (d) mannitol (e), and colony forming units (f) concentration with estimated fluorescent particle mass from UV-APS. Correlation of fungal spore number calculated from arabitol (g), mannitol (h), and colony forming unit (i) concentration with fluorescent particle concentration from WIBS Cluster 1. R^2 value shown for each fit (right two columns). Linear fit parameters are shown in Table S3.
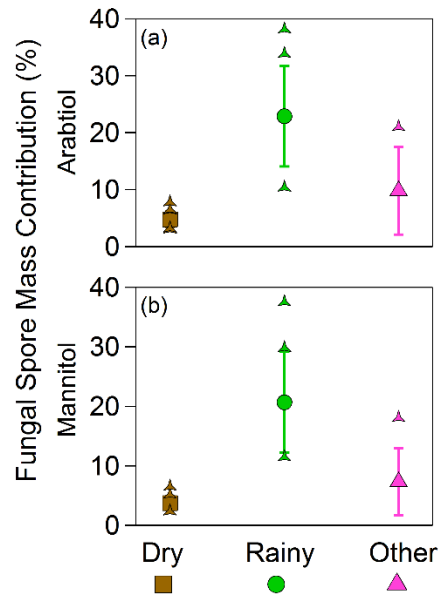
1061
1062 **Figure 7:** Estimated fraction of total aerosol mass contributed by fungal spores. Fungal spore mass
1063 concentration ($\mu g/m^3$) calculated separately from mannitol and arabitol concentration and using average
1064 mass per spore reported by Bauer et al. (2008b). Total particulate matter mass calculated from UV-APS
1065 number concentration (m^{-3}) and converted to mass over aerodynamic particle diameter range $0.5 - 15$ µm
1066 using density of 1.5 g cm^{-3}. Central marker shows mean value of individual filter concentration values,
1067 bars represent standard deviation (*s*) range of filter values, and individual points show outliers beyond
1068 mean $\pm$ *s*.

1069
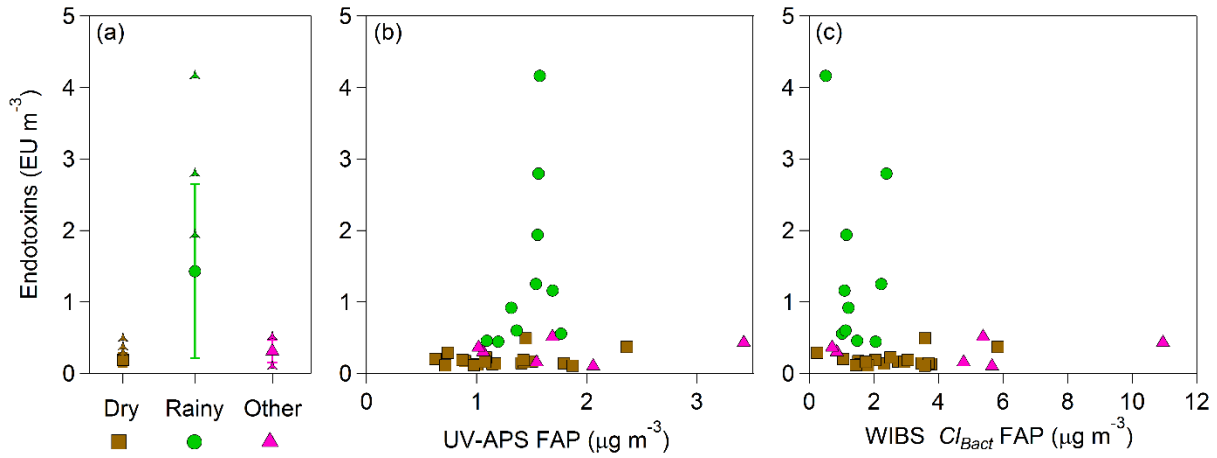
1070
1071
1072 **Figure 8**: Endotoxin mass concentration as an approximate indicator of gram-negative bacteria
1073 concentration. (a) Averaged concentration in each wetness category. Central marker shows mean value of
1074 individual filter concentration values, bars represent standard deviation (*s*) range of filter values, and
1075 individual points show outliers beyond mean ± *s*. (b) Correlation of endotoxin mass concentration with
1076 estimated fluorescent particle mass from UV-APS. (c) Correlation of endotoxin mass concentration with
1077 estimated fluorescent particle mass summed from Clusters 2, 3, and 4 from Crawford et al. (2015).